Integrative computational approach identifies new targets in CD4+ T cell-mediated immune disorders

Bhanwar Lal Puniya[1], Bailee Lichter[1*], Robert Moore[1*], Alex Ciurej[1], Sydney Townsend[1], Ab Rauf Shah[1], Matteo Barberis[2‡§], Tomáš Helikar[1‡§]

[1]Department of Biochemistry, University of Nebraska-Lincoln, USA

[2]Systems Biology, School of Biosciences and Medicine, Faculty of Health and Medical Sciences, University of Surrey, UK

***These authors contributed equally to this work**

‡ These authors are joint senior authors and contributed equally to this work

§To whom correspondence should be addressed:

Matteo Barberis, Ph.D., Systems Biology, School of Biosciences and Medicine, Faculty of Health and Medical Sciences, University of Surrey, UK. Email: matteo@barberislab.com or m.barberis@surrey.ac.uk

Tomáš Helikar, Ph.D., Department of Biochemistry, University of Nebraska-Lincoln, USA, Email: thelikar2@unl.edu

Abstract:

CD4+ T cells, which provide adaptive immunity against pathogens and abnormal cells, are also associated with various immune related diseases. CD4+ T cells' metabolism is dysregulated in these pathologies and represents an opportunity for drug discovery and development. However, we currently lack clear view of the target space in this area. Genome-scale metabolic modeling offers an opportunity to accelerate drug discovery by providing high-quality information about

possible target space in the context of a modeled disease. Here, we develop genome-scale models of naive, Th1, Th2 and Th17 CD4+ T cell subtypes to map metabolic perturbations in three autoimmune disease, rheumatoid arthritis, multiple sclerosis, and primary biliary cholangitis. We subjected these models to *in silico* simulations for drug response analysis of existing FDA-approved drugs, and compounds. Integration of disease-specific differentially expressed genes with altered reactions in response to metabolic perturbations identified 68 drug targets for the three autoimmune diseases. Modulation of forty percent of these targets has been observed to lead to suppression of CD4+ T cells, further increasing their potential impact as therapeutic interventions.

Introduction:

CD4+ T cells are essential components of the human immune system that fight against pathogenic invaders and abnormal cells by producing cytokines, and stimulating other cells, such as B cells, macrophages, and neutrophils (Zhu and Paul, 2008). During immune response, CD4+ T cells are activated and proliferate, and their metabolism adjusts to fulfill increased bioenergetic and biosynthetic demands. For example, activated effector CD4+ T cells are highly glycolytic (Michalek et al., 2011) and use aerobic glycolysis and oxidative phosphorylation (OXPHOS) for proliferation (Chang et al., 2013). On the other hand, naïve, resting, and regulatory CD4+ T cells are less glycolytic and use OXPHOS and fatty acid oxidation (FAO) for energy generation. Accordingly, metabolically dysregulated CD4+ T cells were observed in several diseases such as diabetes (Granados et al., 2017), atherosclerosis (Lü et al., 2018), cancers (Le Bourgeois et al., 2018), and autoimmune diseases such as rheumatoid arthritis (RA) (Okano et al., 2018; Yang et al., 2013), multiple sclerosis (MS) (Gerriets et al., 2015), primary biliary cholangitis (PBC) (Jones, 1996), and systemic lupus erythematosus (SLE) (Yang et al., 2015; Yin et al., 2015). Furthermore, metabolism of Type 1 T helper (Th1), Type 17 T

helper (Th17), and inducible regulatory T cells have been found to be dysregulated in MS (Hedegaard et al., 2008). Controlling CD4+ metabolic pathways can be important in fighting against some immune diseases. For example, CD4+ T cells are hyperactive in systemic lupus erythematosus (SLE), and inhibiting glycolysis as well as the mitochondrial metabolism improved the outcome in an animal model (Yin et al., 2016). Together, this evidence suggests a significant role of CD4+ T cell metabolism in immune-mediated diseases.

Repurposing existing drugs for novel indications represents a cost-effective approach for the development of new treatment options (Pushpakom et al., 2019). Several studies have recently demonstrated the potential for drug repurposing in CD4+ T cell-mediated diseases (Bettencourt and Powell, 2017; Soria-Castro et al., 2019). For example, 2-deoxy-D-glucose (anticancer agent) and metformin (antidiabetic drug) were shown to reverse SLE in a mouse model (Yin et al., 2016). However, drug repurposing, as well as drug discovery and development efforts for targeting T cell metabolism have been limited due the lack of knowledge about the key molecular targets in this context.

In recent years, analysis of large-scale biological datasets has emerged as a powerful strategy for discovery of novel mechanisms, drug targets, and biomarkers in human diseases (Geyer et al., 2017; Puniya et al., 2013, 2016b, 2016a). Here, we develop a computational modeling approach that integrates multi-omic data with systematic perturbation analyses of newly constructed whole-genome metabolic models of naïve CD4+ T cells, and Th1, Th2, and Th17 cells. This led to identification of potential drug targets for CD4+ T cell-mediated diseases (RA, MS, and PBC).

Results

Identification of genes expressed in the CD4+ T cells

We used the computational approach shown in Fig.1 (see also *Supplementary Methods 1*) to construct metabolic models of naïve and effector CD4+ T cells. To identify metabolic genes expressed across CD4+ T cell subtypes (Naïve, Th1, Th2, and Th17 cells), we integrated transcriptomics and proteomics data (*Supplementary Data 1*). The comparison of genes expressed in CD4+ T cell subtypes identified by different datasets are shown in *Supplementary Figure 1*. The analysis showed that between 675 and 836 metabolic genes were expressed depending on the CD4+ T cell subtype (*Supplementary Data 2*). Of these, 530 genes were expressed in all subtypes (Fig. 2a). On the other hand, 16, 25, 7, and 96 genes were specific to naïve, Th1, Th2, and Th17 cells, respectively. Pathway enrichment analysis using active metabolic genes suggested 6 enriched KEGG pathways common across all subtypes: carbon metabolism, TCA cycle, oxidative phosphorylation (OXPHOS), amino sugar and nucleotide sugar metabolism, and valine, leucine and isoleucine degradation (Fig. 2b). Fatty acid degradation and pentose phosphate pathway were enriched in naïve CD4+ T cells only, and fatty acid metabolism was enriched in the naïve, Th2, and Th17 subtypes. No specific KEGG pathways were found enriched solely in Th1, and Th17 cells. Among the enriched pathways shared by all CD4+ T cells, TCA cycle was enriched more than two-fold in naïve, Th1, and Th2 subtypes. Similarly, OXPHOS was enriched more than two-fold in naïve and Th1 subtypes (Fig. 2c). These results suggest that key metabolic pathways are active across all the subtypes. Importantly, the metabolism of various CD4+ T cell subtypes can be different with respect to these pathways' levels of activity and the number of reactions active within the pathways.

Development and validation of genome-scale metabolic models of CD4+ T cells

To further examine these issues, we developed constraint-based metabolic models specific to naïve CD4+ T cells, Th1, Th2, and Th17 cells. Our genome-scale metabolic models comprised of 3,956 to 5,282 reactions associated with 1,055 to 1,250 genes (Table 1; *Supplementary Dataset 1)*. The number of internal enzyme-catalyzed reactions were 2,501, 1,969, 2,549, and 2,640 for naïve, Th1, Th2, and Th17 models respectively, distributed across 84 metabolic pathways (*Supplementary Figure 2; note that transport and exchange reactions were excluded*). The models include more genes associations than active genes identified from the data because the model-building algorithm inserts some reactions that are not supported by data but required for the model to achieve essential metabolic functions for biomass production (see *STAR Methods*).

We validated the models based on the active pathways and gene essentiality. We first identified pathways that are known to be active in different CD4+ T cell subtypes (see *STAR Methods*) and searched for their activity (with non-zero fluxes) in the corresponding models through Flux Balance Analysis (FBA). Several major pathways were in agreement with the literature. These include glycolysis, TCA cycle, glutaminolysis and pyruvate to lactate conversion (aerobic glycolysis) that showed non-zero flux in all the models (Fig. 3 a-d). Effector CD4+ T cells (Th1, Th2, and Th17) showed more flux through fatty acid biosynthesis and less flux through fatty acid β oxidation than naïve CD4+ T cells. A schematic representation of all major pathways active across CD4+ T cells is shown in Fig. 4a. Also, in all the models, limiting glucose from the environment resulted in decreased growth rate (Fig. 4b). It's important to note that the activity of some pathways in the models was not in agreement with the literature. Specifically, we did not observe a significant effect on growth rate when glutamine (Buck et al., 2015) was removed from exchange reactions in the effector CD4+ T cell models (Fig. 4c). This discrepancy can be

explained by the presence of functional glutamine synthase (GLNS) that can convert glutamate to glutamine in the absence of glutamine uptake in the model. We also observed that the growth rate of naïve CD4+ T cells was more dependent on the glucose and glutamine uptake than in the other subtypes (Fig. 4b - d), which is also not in agreement with the literature.

Next, we validated essential genes predicted by models against independent data. Gene deletion analysis predicted 84, 95, 81, and 84 genes as essential in the naïve, Th1, Th2, and Th17 models respectively (*Supplementary Data 3*). More than 70% of these predictions agreed with genes experimentally defined as essential and conditionally essential (Chen et al., 2017). The models achieved an accuracy (ratio of *true positives* and *true negatives* to the whole pool) of ~60% and precisions (ratio of *true positives* to *true positives* and *false positives*) ranging from 72% to 75% (*Supplementary Figure 3*). Additional validations based on CD4+ T cell-specific essential functions are presented in *Supplementary Methods 3*. Overall, the validation confirmed that our constraint-based metabolic models specific to naïve CD4+ T cells, Th1, Th2, and Th17 cells represent relevant and realistic systems to examine drug response and predict drug targets.

Mapping existing, and identifying potential drug targets in CD4+ T cells

We used the validated CD4+ T cell-specific models to predict potential drug targets and combined it with the publicly available drug repurposing and tool compound data set from the Connectivity Map (cMap) database and mapped the approved drugs, clinical drug candidates and tool compounds in the dataset with the metabolic genes in the models (Fig. 5a). Next, we performed *in silico* knock-outs of the associated drug target genes. Due to the presence of isozymes, not all the deleted target genes influenced the reaction(s). We identified 86, 79, 86, and 90 target genes whose deletion blocks at least one reaction in naïve, Th1, Th2, and Th17

models, respectively (Fig. 5b). Of these, 62 were common among four CD4+ T cell subtypes (Fig. 5c). Twenty-five genes were targets only in Th1 cells. All modeled gene deletions resulted in altered flux distributions that were quantified using flux ratios. For each drug target deletion, we classified all reactions into three categories (see *STAR Methods*): (1) reactions with decreased fluxes (down-reactions), (2) reactions with increased fluxes (up-reactions), and (3) reactions without any changes. We used these flux ratios to identify potential drug targets specific for immune diseases, by exploring how disease-specific metabolic functions are affected upon each drug target inhibition.

First, we identified disease-specific metabolic functions for RA, MS, and PBC using differential gene expression analysis of publicly available patients' data (Case-Control studies) (see *STAR Methods*). We identified 852, 1,459, and 553 differentially expressed genes (DEGs) for RA, MS, and PBC, respectively (*Supplementary Data 4*). From these DEGs, we selected genes relevant to our metabolic models. For example, 36 metabolic genes were upregulated and 27 genes were downregulated in RA (Fig. 6a). Biological process enrichment analysis identified purine metabolism, and starch sucrose metabolism as enriched in upregulated genes. On the contrary, lysine degradation, fatty acid elongation, and carbon metabolism were downregulated. Enriched metabolic pathways for all three diseases are shown in *Supplementary Data 4*.

To identify potential drug targets for the aforementioned diseases, we looked for target genes whose deletion (inhibition) would have the appropriate effect on diseases' DEGs. For each gene inhibition, we specifically investigated the decrease in metabolic flux through reactions controlled by genes upregulated in disease, and increase in metabolic flux through reactions controlled by genes downregulated in disease (Fig. 6b). Using flux ratios of metabolic DEGs, we calculated a *perturbation effect score* (PES; see *STAR Methods*) for each drug target gene in

each pair model/disease. PES represents the effect of gene inhibition on both upregulated and downregulated genes. A positive PES value for the drug target gene means that its inhibition decreases more fluxes controlled by genes upregulated in disease than it increases or increases more fluxes controlled by genes downregulated in disease than it decreases. As such, inhibition of that gene target reverses the fluxes controlled by disease DEGs. In contrast, a negative PES means that the inhibition of a target gene increases more fluxes controlled by upregulated genes or decrease the more fluxes controlled by downregulated genes than the opposite. Among the different combinations of cell types and diseases, the PESs range was from -2 to 2 (*Supplementary Figure 4*). Based on these considerations, genes with higher positive PES can serve as potential drug targets for the disease.

Using PES as a measure of target relevance, we identified 62 potential drug targets that were common to our models (Fig. 5c). These genes displayed various PES ranks across models and diseases. To choose drug targets that performed better across different CD4+ T cells, we considered PES ranks of the four subtype-specific models. First, we normalized the PES ranks by transforming them to Z-scores in each model. Since the studied diseases typically involve more than one type of CD4+ T cell subtype, we next summed up the Z-scores of all the models within a disease for each drug target (*Supplementary Figure 4*). A minimum aggregate Z-score represents overall high PES ranks predicted across four cell types. Therefore, a gene with a minimum aggregated Z-score could be a potential high confidence drug target. We used a Z-score cutoff of -1 (1 standard deviation lower than the mean aggregated Z-score) and identified 17, 27, and 24 potential drug targets for RA, MS, and PBC, respectively (Table 2). Ranking based on aggregated Z-scores is provided in *Supplementary Data 5*. Taken together, our combined use of the disease-matched genome-scale metabolic models of CD4+ T cells and

the well target-annotated public dataset of bioactive compounds generated a manageable list of potential drug targets suitable for deeper analysis and follow-up.

Analysis and validation of predicted drug targets

To further analyze and validate our target list, we performed a comprehensive literature survey (Table 2). Among the 17 suggested drug targets for RA, dihydroorotate dehydrogenase (DHODH) and Acetyl-CoA acetyltransferase (ACAT1) have been already explored as targets in drug development efforts (Breedveld and Dayer, 2000; Tian et al., 2011), and 15 genes were newly identified. Among these, eight (LSS, NAMPT, FDPS, SQLE, EPHX2, CAT, CS, SOD2) have been found to inhibit CD4+ T cell proliferation upon deletion (Table 2). The product of the reaction catalyzed by 4-Aminobutyrate Aminotransferase (ABAT) is linked to RA. Dysregulation of other genes, such as pyruvate dehydrogenase E1 (PDHB), Farnesyl-diphosphate farnesyltransferase 1 (FDFT1), Oxoglutarate Dehydrogenase (OGDH), alpha- galactosidase (GAA), has not been previously reported to impact CD4+ T cell proliferation.

Furthermore, we predicted 27 possible drug targets for MS. Of these, glutathione reductase (GSR), and dihydrofolate reductase (DHFR) were already explored as targets using the experimental autoimmune encephalomyelitis (EAE) model (Ashtari and Savoj, 2011; Lian et al., 2018) and 25 genes were newly identified. Among these, 12 (CAT, IDH2, HMGCR, PKM, ABAT, LSS, FASN, PPAT, PNP, CS, CAD, SQLE) have been previously reported to inhibit CD4+ T cell proliferation upon deletion. Genes that were not previously reported to affect CD4+ T cells upon deletion include Carnitine O-palmitoyltransferase 2 (CPT2), MP cyclohydrolase (ATIC), Ornithine decarboxylase (ODC1), Dihydropyrimidine dehydrogenase (DYPD), and Farnesyl-diphosphate farnesyltransferase (FDFT1).

Finally, we identified 24 possible drug targets for PBC. None of them was previously explored as a drug target in PBC. Deletion of seven of these potential gene targets (NAMPT, EPHX2, FASN, ADA, SLC2A3, TXNRD1, ACLY) has been reported to affect CD4+ T cells in the literature. Genes that have not yet been reported to affect CD4+ T cells upon deletion include Long-chain-fatty-acid--CoA ligase 3 (ACSL3), Adenosine kinase (ADK), and S-adenosylmethionine decarboxylase proenzyme (AMD1).

Some of the 68 predicted drug targets were shared by diseases but 55 were unique: six drug targets (LSS, ABAT, SQLE, FDFT1, CAT, CS) were in common between RA and MS; five drug targets (NAMPT, EPHX2, COMT, HIBCH, GAA) were in common between RA and PBC; and two drug target (ADH5, FASN) were in common between MS and PBC. Drugs and compounds available for these targets are shown in Table 3.

Taken together our analysis has identified 68 possible drug targets of relevance to metabolic regulation of autoimmune diseases. We discuss implications of our results in more detail below.

Discussion

Our predicted drug targets were classified into two categories: validated, and novel. We considered a target to be validated if previously explored as such in the context of RA, MS and/or PBC. Novel targets, those not previously reported as such for the three diseases we focused on here, were further classified into two subcategories: target genes that are supported with published experimental data, and predicted target genes for which no data is currently available. We will discuss select examples of targets in each of these categories to illustrate ways in which our model and analysis can be used to advance future drug repurposing as well as drug discovery efforts.

Our predictions include three genes (*DHODH*, ACAT1, and *DHFR*) that code for proteins targeted by approved drugs currently used for treatment of autoimmune diseases (Ashtari and Savoj, 2011; Breedveld and Dayer, 2000; Kumar and Banik, 2013; Lian et al., 2018; Tian et al., 2011). A strong example of an already validated drug target predicted by our models is dihydroorotate dehydrogenase (DHODH), a key enzyme in de novo pyrimidine synthesis pathway, and a target of leflunomide, an approved drug for rheumatoid arthritis (Breedveld and Dayer, 2000; Li et al., 2004). DHFR (dihydrofolate reductase) is a well-established oncology drug target, and also as an immunosuppressant and anti-inflammatory target (Schweitzer et al., 1990). Low doses of an FDA-approved DHFR inhibitor methotrexate have been found effective as a treatment for MS, RA, and Crohn's disease (Ashtari and Savoj, 2011). Mitochondrial acetyl-CoA acetyltransferase (ACAT1) is a target for FDA approved anti-inflammatory drug sulfasalazine in inflammatory bowel syndrome. Furthermore, this drug is indicated for treatment for rheumatoid arthritis and ulcerative colitis (Wishart et al., 2018). Taken together, our models successfully replicated current clinical practice, further strengthening the value of our approach.

Interestingly, a major subcategory of gene targets we identified code for proteins that have not previously been explored for treatment of RA, MS, and PBC. We can now use these insights to formulate novel preclinical and clinical hypothesis. For example, *ABAT*, which encodes the GABA-transaminase enzyme that breaks down γ-aminobutyric acid (GABA; a neurotransmitter), was identified in our analysis as a potential target. While ABAT has not been previously identified as a drug target for RA, we can hypothesize that its inhibition may increase free GABA levels which would, in turn, inhibit CD4+ T cell activation. The relationship between GABA levels and suppressions of CD4+ T cell activation has been previously reported, further suggesting a link between neurotransmission and immune response (Bhandage et al., 2018; Jin et al., 2013;

Mendu et al., 2012). There are currently two FDA approved drugs, vigabatrin and phenelzine, that target ABAT. Although we don't expect that either one of these agents can be repurposed to treat autoimmune disease given that they are an anti-seizure medicine and an antidepressant, respectively, we propose that further analysis of relationships between neurotransmission and immune response offers an interesting targeting opportunity (Tian et al., 2011). Another example is glutathione reductase (GSR), an enzyme that reduces oxidized glutathione disulfide to cellular antioxidant GSH (Safran et al., 2010). It has been shown that inhibition of the de novo GSH synthesis can reduce the pathological progression of experimental autoimmune encephalomyelitis (EAE) (Lian et al., 2018). Here, carmustine, a chemotherapy drug, is FDA approved drug that targets GSR, offering a viable starting point for future pre-clinical testing (Table 3). Additional high confidence predictions and target candidates are a group of genes that have been experimentally shown to repress CD4+ T cells upon inhibition. This list includes nicotinamide phosphoribosyltransferase (NAMPT), which we now predict is a drug target for RA. This enzyme is involved in NAD+ synthesis (The UniProt Consortium, 2017) and was previously explored as a drug target in EAE for MS (Bruzzone et al., 2009), melanoma, T cell lymphoma, and leukemia (Roulston and Shore, 2016). Given that two NAMPT inhibitors, GMX1778 and FK-866, are in phase II clinical trials (Table 3), this enzyme represents a target where pre-clinical testing and follow up may lead to drug repurposing opportunities. Another example worth highlighting is epoxide hydrolase 2 (EPHX2), which converts toxic epoxides to non-toxic dihydrodiols (Safran et al., 2010; The UniProt Consortium, 2017). Its inhibition was reported to result in decreased production of proinflammatory cytokines in preclinical evaluation in inflammatory bowel syndrome (Reisdorf et al., 2019). For EPHX2, an inhibitor GSK2256294A is in phase I clinical trial, indicating that developing drugs for this target may be possible. Moreover, our model implicated enzymes such

as pyruvate kinase (PKM), which impacts glycolysis, HMG-CoA reductase (HMGCR), which regulates cholesterol biosynthesis and adenosine deaminase (ADA), which converts harmful deoxyadenosine to not harmful deoxyinosine. Each one of these enzymes has been experimentally linked to T cell proliferation and development (Alves-Filho and Pålsson-McDermott, 2016; Bietz et al., 2017; Flinn and Gennery, 2018), and all three targets have been the subject of previous drug development campaigns (Table 3). ATP Citrate Lyase (ACLY), Catalase (CAT), Farnesyl diphosphate synthase (FDPS), Lanosterol synthase (LSS), Squalene epoxidase (SQLE), and Superoxide dismutase 2 (SOD2) also represent targets we identified. SQLE is involved in cholesterol biosynthesis, and in general agreement with recent reports that inhibiting cholesterol pathways can suppress T cell proliferation (Bietz et al., 2017). The loss of SOD2 can increase superoxides and defective T cell development (Case et al., 2011). For all these targets, either preclinical, clinical or approved inhibitors are available, which we consider encouraging for further study and drug repurposing (see Table 3 for details).

Other predicted genes are part of the TCA cycle (Citrate synthase (CS), Isocitrate dehydrogenase 2 (IDH2)), ribonucleotide biosynthetic processes (Phosphoribosyl pyrophosphate amidotransferase (PPAT), Carbamoyl-phosphate synthetase 2, Aspartate transcarbamylase, and Dihydroorotase (CAD)), and lipid biosynthesis (Fatty acid synthase (FASN)) that are also important for T cell development. As with examples above, many of these potential candidate targets have inhibitors that are in different stages of preclinical and clinical development, and some (like PPAT and FASN inhibitors) have been FDA approved (Table 3).

Furthermore, in addition to gene targets with robust or partial experimental evidence, we identified 31 novel gene targets for which no evidence currently exists. These genes are involved in glycolysis, TCA cycle, OXPHOS, fatty acid metabolism, pyruvate metabolism, purine,

and pyrimidine metabolism, arginine and proline metabolism,and tyrosine metabolism pathways, which are critical for T cell activation and proliferation (Almeida et al., 2016; Wang and Green, 2012). Collectively, our models led to identification of potential high-value targets for RA, MS and PBC treatment, and implicated several drugs in current clinical use for drug repurposing.

We would also like to discuss several more technical points regarding our approach. Data integration enabled us to build, refine, and validate high-quality cell type-specific models. While many of the major pathways important for CD4+ T cell activation and proliferation are commonly active across different CD4+ T cell subtypes we tested, the models differ with respect to how these pathways are used for growth. For example, higher activity of the fatty acid oxidation pathway is more important in naïve but not in effector CD4+ T cells that have elevated glycolysis (Wang and Green, 2012) and fatty acid synthesis pathways. These models achieved ~60% accuracy with gene essentiality data obtained from different cell lines (Chen et al., 2017), which might further improve with the availability of CD4+ T cell-specific essentiality data. Integration of disease-associated DEGs with flux profiles under gene knock-out helped us to select disease-specific drug targets. While computational models of signal transduction in CD4+ T cells (Carbo et al., 2013; Puniya et al., 2018) are available, metabolic models of effector and regulatory CD4+ T cells have not been developed (except for naïve CD4+ T cells (Han et al., 2016)). Similar metabolic models were previously used to predict drug targets against pathogens (Puniya et al., 2013) and complex diseases such as cancers (Jerby and Ruppin, 2012).

While our approach can be generalized for human diseases and used with any -omics dataset, the unavailability of reliable data contributes to some limitations. Because of heterogeneity with

respect to time after stimulation with cytokines in the available datasets, constructed models represent inclusive metabolic phenotypes during activation and proliferation for each CD4+ T cell subtype. Thus, time-specific data would be required to study metabolic phenotype at a specific time point in CD4+ T cell development. In addition, the biomass objective function used in our study is not specific to CD4+ T cells. A specific objective function that considers varying utilization of precursor metabolites (such as glycolysis intermediates) by different CD4+ T cells for biomass production, might further improve the models. However, we have shown that changing objective functions (from the Recon3D to macrophage model) had no significant impact on the constructed models (see STAR Methods for details). Similarly, reliable disease-specific data were unavailable for specific CD4+ T cell subtypes, therefore, building subtype specific cell metabolic models under disease conditions was not possible. We mitigated this limitation by integrating disease-specific DEGs from sorted CD4+ T cells with models, which resulted in metabolic fluxes relevant to diseases. In the future, with the availability of more disease and cell type-specific data, our integrative approach may further improve these results.

Overall, our integrative systems modeling approach has provided a new perspective for the treatment of RA, MS, and PBC. Moreover, the newly constructed models may serve as tools to explore metabolism of CD4+ T cells. Additionally, our approach is generalizable to other disease areas for which reliable disease-specific data are available, making it a potentially important computational platform for both novel drug target identification, as well as prioritizing targets for drug repurposing efforts.

STAR Methods

High throughput data acquisition and integration

We collected transcriptomics data from the GEO (Barrett et al., 2013) database and proteomics data (Rieckmann et al., 2017). A total of 121 transcriptomics (Abbas et al., 2005; Bernier et al., 2013; Bonacci et al., 2012; Gustafsson et al., 2015; Kleinewietfeld et al., 2013; Lund et al., 2003; Prots et al., 2011; Santarlasci et al., 2012; Zhang et al., 2013) and 20 proteomics (Rieckmann et al., 2017) samples relevant to the CD4+ T cells were selected (*Supplementary Data 1*). Transcriptomics data analysis was performed using the *affy* (Gautier et al., 2004) and *limma* (Ritchie et al., 2015) R packages. Because we aimed to characterize gene activities instead of gene expression levels, the processed transcriptomics data were discretized (active = 1; inactive = 0) and samples for each cell type were combined together. Genes active in more than 50% of the samples in which the probe was present were considered as active (*see Supplementary Methods 2*). Similarly, proteins expressed in more than 50% of samples in the proteomics dataset were considered as active. In the proteomics datasets, protein IDs were mapped to gene IDs.

Next, we integrated activities from transcriptomics and proteomics datasets. First, biological entities that overlapped in both types of data were selected as high-confidence. Second, we found that some genes were expressed in the majority of transcriptomics datasets, but expressed in less than 50% samples of proteomics data. Similarly, some proteins were identified within groups of highly abundant proteins in multiple samples in proteomics datasets but expressed in less than 50% samples of transcriptomics datasets. Such non-overlapping genes were selected as moderate-confidence based on consensus in single types of -omics data (*Supplementary Methods 2.1.1*). Third, moderate-confidence genes exclusively present in the transcriptomics data were added to the overlapping genes if expressed in at least 90% of samples. Fourth, moderate-confidence genes exclusively present in the proteomics dataset

were added if their abundance was ranked in the top 25% (fourth quartile) (*Supplementary Methods 2; Supplementary Data 6*). We used these cutoffs to decrease the false negatives while not selecting false positives by removing genes and proteins that are not expressed in any sample either in transcriptomics or proteomics data.

Cell type-specific genome-scale metabolic model reconstruction

We used the GIMME (Becker and Palsson, 2008) method (in COBRA toolbox) to construct the metabolic models of different CD4+ T cells (naïve, Th1, Th2, Th17). The inputs for GIMME were the generic human Recon3D (Brunk et al., 2018) (as a template) and gene expressions based on integrated multi-omics data. The template Recon3D was modified prior to constructing CD4+ T cell-specific metabolic models. These modifications included gene-protein-reaction (GPR) associations (all genes associated with a reaction written using AND and OR operators), media conditions, and reaction directionality. In addition, new reactions involved in the biomass objective function were added, and some reactions were removed as described below (See also *Supplementary Methods 2*). The used transcriptomics and proteomics data have information about genes/proteins instead of transcript variants. To map the data obtained for genes, we updated transcript IDs provided in Recon3D to Entrez gene IDs. A total of 1,892 genes were included in the modified Recon3D model. Furthermore, because different CD4+ T cells have different nutrient uptake preferences, we used two types of media conditions (one for each naïve and one for all effector T cells). For all cell subtypes, in addition to the basal metabolites (unconstrained and freely available, i.e. H2O, O2, H, O2S, CO2, Pi, H2O2, HCO3, H2CO3, and CO), glucose, glutamine, and other amino acids were set as open (un-constrained) for uptake. Furthermore, the directionality of some reactions was updated based on the Recon 2.2.05 model (Swainston et al., 2016). Because of the lack of CD4+ T cell-specific data, the biomass

objective function was adopted from the macrophage model iAB-AMØ-1410 (Bordbar et al., 2010) and added to the Recon3D.

For each subtype, we constructed three models based on transcriptomics, proteomics, and integrated (transcriptomics and proteomics data) datasets. A comparison of these models is provided in *Supplementary Figure 5* and details can be found in *Supplementary Methods 2*. The models constructed with integrated data were selected for further analysis. Additionally, to investigate the effect of biomass objective function on constructed models, we built two models using biomass objective functions from (1) Recon3D and (2) iAB-AMØ-1410 models. The reactions in output models generated based on each biomass function were compared. The models based on the two objective functions were not significantly different (*Supplementary Figure* 6) with respect to the numbers of reactions. Biomass objective function from iAB-AMØ-1410 consists of few extra precursors that predicted better fluxes through fatty acid pathways. Therefore models that are constructed based on biomass reaction adopted from iAB-AMØ-1410 were used in subsequent analyses. Models were further reduced by removing the dead-end reactions. Reactions in the models are distributed across different compartments including extracellular, cytoplasm, mitochondria, nucleus, Golgi apparatus, lysosome, and endoplasmic reticulum. The models were investigated to perform basic properties using leak test, gene deletion and further refined in an iterative manner. Refined models were then subjected to 460 metabolic tasks that were used with the Recon3D model and included in *Test4HumanFctExt* function in COBRA (*Supplementary Data 7*). The constructed models were simulated using Flux Balance Analysis (FBA) and Flux Variability Analysis (FVA). The final numbers of metabolites and reactions are presented in Table 1. These models were named as TNM1055 (naïve model), T1M1133 (Th1 model), T2M1127 (Th2 model), and T17M1250 (Th17 model) and can be found as *Supplementary Dataset 1*. They have also been submitted to

BioModels database (Chelliah et al., 2015) under accessions MODEL1909260003, MODEL1909260004, MODEL1909260005, MODEL1909260006.

Model validation

Models were validated based on literature knowledge related to active pathways and gene essentiality data. CD4+ T cell-specific metabolic functions were searched in the literature using PubMed (Sayers et al., 2019). Naïve CD4+ T cells tend to have low energy demands, and mainly rely on *fatty acid β-oxidation*, oxidation of pyruvate and glutamine via the *TCA cycle* (Patsoukis et al., 2016). On the other hand, the high bioenergetics demand in effector cells is met by shifting *OXPHOS* to *glycolysis* and *fatty acid oxidation* to *fatty acid synthesis* (Almeida et al., 2016). Furthermore, similar to cancer cells, proliferating effector CD4+ T cells convert lactate from pyruvate by lactate dehydrogenase enzyme (Almeida et al., 2016). Thus, we obtained the flux distribution of metabolic pathways under wild type conditions using Flux Balance Analysis (FBA) and searched the non-zero fluxes through the aforementioned pathways in all the models. Flux maps were created using Escher web application (https://escher.github.io/#/) (King et al., 2015; Rowe et al., 2018). It has also been observed previously that deficiency in glucose and glutamine impairs CD4+ T cell activation and proliferation (Macintyre et al., 2014; Ren et al., 2017). We performed this experiment *in silico*, whereby we varied the flux through exchange reactions of glucose (EX_glc[e]) and glutamine (EX_gln_L[e]) in the models and analyzed the effect on growth rate. To perform gene essentiality-based validation, we knocked out model genes to predict their effect on the growth rate. This was performed using *singleGeneDeletion* in the COBRA toolbox using the Minimization of Metabolic Adjustment (MoMA) method (Segrè et al., 2002). Because of the unavailability of CD4+ T cell-specific data, predicted essential genes were compared with experimentally identified essential genes in humans from different cell lines. The data for experimentally tested essential and nonessential genes for human were

obtained from the OGEE database (Chen et al., 2017). In this database, the essentiality data for humans was compiled using 18 experiments across various cell lines that include RNAi based inhibition, CRISPR, and CRISPR-CAS9 systems. To calculate the predictive power of the model, predicted essential genes were compared with experimentally observed essential and conditionally essential genes reported in the OGEE database. Essential and conditionally essential genes were merged together. Additional validations of models using CD4+ T cell-specific essential genes can be found in *Supplementary Methods 3*.

Mapping drug targets

The developed models were used to predict potential drug targets for autoimmune diseases in which effector subtypes have been found hyperactive (Hoyer et al., 2009; Ivanova and Orekhov, 2015). Therefore, a reasonable drug target should downregulate effector CD4+ T cells. Among the metabolic genes of selected models, we first identified targets of existing drugs. The drugs and their annotations including target genes were imported from The Drug Repurposing Hub (Corsello et al., 2017) in the ConnectivityMap (CMap) database (Subramanian et al., 2017). All withdrawn drugs and their annotations were first removed. In this list, the gene symbols of target genes of drugs were converted to Entrez IDs. Next, we searched Entrez IDs from CMap data in the genes of metabolic models. For each mapped gene in the model, the drugs were listed.

Metabolic genes differentially expressed in autoimmune diseases

The lack of reliable data from specific CD4+ T cell subtypes involved in autoimmune disease conditions led us to utilize patients' data (case-control studies) available for autoimmune diseases that were collected from peripheral CD4+ T cells. Datasets GSE56649 (Ye et al., 2015) (rheumatoid arthritis), GSE43591 (Jernås et al., 2013) (multiple sclerosis), and GSE93170 (Nakagawa et al., 2017) (primary biliary cholangitis) were obtained from the GEO

database. Raw data files were processed using the *affy* and *limma* packages (Gautier et al., 2004; Ritchie et al., 2015) in Bioconductor/R. The *limma* package was used to identify DEGs between patients and healthy controls. For significant differential expression, selective cutoffs of fold-changes were used with adjusted P-values < 0.05. For differentially expressed genes, we used a two-fold cutoff. A cutoff of 1.5 fold was used for datasets where two-fold resulted in a very low number to zero differentially expressed metabolic genes.

Perturbation of metabolism and perturbation effect score (PES)

In metabolic models, the knockout of genes that are targets of existing drugs was performed in the COBRA toolbox using MoMA (Segrè et al., 2002). For each knockout, we investigated the change in fluxes regulated by DEGs in diseases. The change in fluxes was computed using flux ratios of perturbed flux/WT flux, and all fluxes that are affected by each perturbation were calculated. We counted fluxes regulated by upregulated genes that are decreased or increased after perturbation (UpDec and UpInc) as well as fluxes regulated by downregulated genes that are decreased or increased after perturbation (DownDec and DownInc). The total number of fluxes for each perturbation also include upregulated genes that were unchanged after perturbation (UpUnc) as well as downregulated genes that were unchanged after perturbation (DownUnc) (see also *Supplementary Methods 7*). For each perturbed gene, a perturbation effect score (PES) was calculated as:

$$PES = \frac{(UpDec - UpInc)}{(UpDec + UpInc + UpUnc)} + \frac{(DownInc - DownDec)}{(DownInc + DownDec + DownUnc)}$$

Next, for each disease and model combination, the ranks of PES were computed. The gene with the highest PES obtained the top rank and the one with the minimum PES obtained the lowest rank. For each disease, we prioritized drug targets by utilizing their ranks across all models. The PES ranks in each model were first transformed into Z-score as:

$$Z - score = \frac{(x - \mu)}{\sigma}$$

where *x* is a PES rank, *μ* is the mean of PES ranks in a model for one disease, σ is the standard deviation of PES ranks obtained by a model for one disease. For each disease type and each gene, Z-scores across four models were summed up to calculate an aggregated Z-score. Genes were ranked based on minimum to maximum aggregate Z-scores.

Pathway enrichment analysis

For biological processes enrichment analysis, we used DAVID V6.8 (Huang et al., 2009), and STRING database (Szklarczyk et al., 2017) together with Gene Ontology biological processes (The Gene Ontology Consortium, 2019), KEGG pathways (Kanehisa et al., 2016), and Reactome pathways (Fabregat et al., 2018). A cutoff of 5% (Boyle et al., 2004; Reimand et al., 2019) False Discovery Rate (FDR) was used for significant enrichment.

References:

Abbas, A.R., Baldwin, D., Ma, Y., Ouyang, W., Gurney, A., Martin, F., Fong, S., van Lookeren Campagne, M., Godowski, P., Williams, P.M., et al. (2005). Immune response in silico (IRIS): immune-specific genes identified from a compendium of microarray expression data. Genes Immun. *6*, 319–331.

Almeida, L., Lochner, M., Berod, L., and Sparwasser, T. (2016). Metabolic pathways in T cell activation and lineage differentiation. Semin. Immunol. *28*, 514–524.

Alves-Filho, J.C., and Pålsson-McDermott, E.M. (2016). Pyruvate Kinase M2: A Potential Target for Regulating Inflammation. Front. Immunol. *7*, 145.

Ando, T., Mimura, K., Johansson, C.C., Hanson, M.G., Mougiakakos, D., Larsson, C., Martins da Palma, T., Sakurai, D., Norell, H., Li, M., et al. (2008). Transduction with the antioxidant enzyme catalase protects human T cells against oxidative stress. J. Immunol. Baltim. Md 1950 *181*, 8382–8390.

Antonioli, L., Colucci, R., La Motta, C., Tuccori, M., Awwad, O., Da Settimo, F., Blandizzi, C., and Fornai, M. (2012). Adenosine deaminase in the modulation of immune system and its potential as a novel target for treatment of inflammatory disorders. Curr. Drug Targets *13*, 842–862.

Arefieva, T.I., Filatova, A.Y., Potekhina, A.V., and Shchinova, A.M. (2018). Immunotropic Effects and Proposed Mechanism of Action for 3-Hydroxy-3-methylglutaryl-coenzyme A Reductase Inhibitors (Statins). Biochem. Biokhimiia *83*, 874–889.

Ashtari, F., and Savoj, M.R. (2011). Effects of low dose methotrexate on relapsing-remitting multiple sclerosis in comparison to Interferon β-1α: A randomized controlled trial. J. Res. Med. Sci. Off. J. Isfahan Univ. Med. Sci. *16*, 457–462.

Bantia, S., and Kilpatrick, J.M. (2004). Purine nucleoside phosphorylase inhibitors in T-cell

malignancies. Curr. Opin. Drug Discov. Devel. *7*, 243–247.
Barrett, T., Wilhite, S.E., Ledoux, P., Evangelista, C., Kim, I.F., Tomashevsky, M., Marshall, K.A., Phillippy, K.H., Sherman, P.M., Holko, M., et al. (2013). NCBI GEO: archive for functional genomics data sets--update. Nucleic Acids Res. *41*, D991-995.
Becker, S.A., and Palsson, B.O. (2008). Context-specific metabolic networks are consistent with experiments. PLoS Comput. Biol. *4*, e1000082.
Bernier, A., Cleret-Buhot, A., Zhang, Y., Goulet, J.-P., Monteiro, P., Gosselin, A., DaFonseca, S., Wacleche, V.S., Jenabian, M.-A., Routy, J.-P., et al. (2013). Transcriptional profiling reveals molecular signatures associated with HIV permissiveness in Th1Th17 cells and identifies peroxisome proliferator-activated receptor gamma as an intrinsic negative regulator of viral replication. Retrovirology *10*, 160.
Bettencourt, I.A., and Powell, J.D. (2017). Targeting Metabolism as a Novel Therapeutic Approach to Autoimmunity, Inflammation, and Transplantation. J. Immunol. Baltim. Md 1950 *198*, 999–1005.
Bhandage, A.K., Jin, Z., Korol, S.V., Shen, Q., Pei, Y., Deng, Q., Espes, D., Carlsson, P.-O., Kamali-Moghaddam, M., and Birnir, B. (2018). GABA Regulates Release of Inflammatory Cytokines From Peripheral Blood Mononuclear Cells and CD4+ T Cells and Is Immunosuppressive in Type 1 Diabetes. EBioMedicine *30*, 283–294.
Bietz, A., Zhu, H., Xue, M., and Xu, C. (2017). Cholesterol Metabolism in T Cells. Front. Immunol. *8*, 1664.
Bonacci, B., Edwards, B., Jia, S., Williams, C.B., Hessner, M.J., Gauld, S.B., and Verbsky, J.W. (2012). Requirements for growth and IL-10 expression of highly purified human T regulatory cells. J. Clin. Immunol. *32*, 1118–1128.
Bordbar, A., Lewis, N.E., Schellenberger, J., Palsson, B.Ø., and Jamshidi, N. (2010). Insight into human alveolar macrophage and M. tuberculosis interactions via metabolic reconstructions. Mol. Syst. Biol. *6*, 422.
Boyle, E.I., Weng, S., Gollub, J., Jin, H., Botstein, D., Cherry, J.M., and Sherlock, G. (2004). GO::TermFinder—open source software for accessing Gene Ontology information and finding significantly enriched Gene Ontology terms associated with a list of genes. Bioinforma. Oxf. Engl. *20*, 3710–3715.
Breedveld, F.C., and Dayer, J.M. (2000). Leflunomide: mode of action in the treatment of rheumatoid arthritis. Ann. Rheum. Dis. *59*, 841–849.
Brunk, E., Sahoo, S., Zielinski, D.C., Altunkaya, A., Dräger, A., Mih, N., Gatto, F., Nilsson, A., Preciat Gonzalez, G.A., Aurich, M.K., et al. (2018). Recon3D enables a three-dimensional view of gene variation in human metabolism. Nat. Biotechnol. *36*, 272–281.
Bruzzone, S., Fruscione, F., Morando, S., Ferrando, T., Poggi, A., Garuti, A., D'Urso, A., Selmo, M., Benvenuto, F., Cea, M., et al. (2009). Catastrophic NAD+ depletion in activated T lymphocytes through Nampt inhibition reduces demyelination and disability in EAE. PloS One *4*, e7897.
Buck, M.D., O'Sullivan, D., and Pearce, E.L. (2015). T cell metabolism drives immunity. J. Exp. Med. *212*, 1345–1360.
Carbo, A., Hontecillas, R., Kronsteiner, B., Viladomiu, M., Pedragosa, M., Lu, P., Philipson, C.W., Hoops, S., Marathe, M., Eubank, S., et al. (2013). Systems modeling of molecular mechanisms controlling cytokine-driven CD4+ T cell differentiation and phenotype plasticity. PLoS Comput. Biol. *9*, e1003027.
Case, A.J., McGill, J.L., Tygrett, L.T., Shirasawa, T., Spitz, D.R., Waldschmidt, T.J., Legge, K.L., and Domann, F.E. (2011). Elevated mitochondrial superoxide disrupts normal T cell development, impairing adaptive immune responses to an influenza challenge. Free Radic. Biol.

Med. *50*, 448–458.
Chang, C.-H., Curtis, J.D., Maggi, L.B., Faubert, B., Villarino, A.V., O'Sullivan, D., Huang, S.C.-C., van der Windt, G.J.W., Blagih, J., Qiu, J., et al. (2013). Posttranscriptional control of T cell effector function by aerobic glycolysis. Cell *153*, 1239–1251.
Chelliah, V., Juty, N., Ajmera, I., Ali, R., Dumousseau, M., Glont, M., Hucka, M., Jalowicki, G., Keating, S., Knight-Schrijver, V., et al. (2015). BioModels: ten-year anniversary. Nucleic Acids Res. *43*, D542-548.
Chen, W.-H., Lu, G., Chen, X., Zhao, X.-M., and Bork, P. (2017). OGEE v2: an update of the online gene essentiality database with special focus on differentially essential genes in human cancer cell lines. Nucleic Acids Res. *45*, D940–D944.
Corsello, S.M., Bittker, J.A., Liu, Z., Gould, J., McCarren, P., Hirschman, J.E., Johnston, S.E., Vrcic, A., Wong, B., Khan, M., et al. (2017). The Drug Repurposing Hub: a next-generation drug library and information resource. Nat. Med. *23*, 405–408.
Fabregat, A., Jupe, S., Matthews, L., Sidiropoulos, K., Gillespie, M., Garapati, P., Haw, R., Jassal, B., Korninger, F., May, B., et al. (2018). The Reactome Pathway Knowledgebase. Nucleic Acids Res. *46*, D649–D655.
Flinn, A.M., and Gennery, A.R. (2018). Adenosine deaminase deficiency: a review. Orphanet J. Rare Dis. *13*, 65.
Gaulton, A., Hersey, A., Nowotka, M., Bento, A.P., Chambers, J., Mendez, D., Mutowo, P., Atkinson, F., Bellis, L.J., Cibrián-Uhalte, E., et al. (2017). The ChEMBL database in 2017. Nucleic Acids Res. *45*, D945–D954.
Gautier, L., Cope, L., Bolstad, B.M., and Irizarry, R.A. (2004). affy--analysis of Affymetrix GeneChip data at the probe level. Bioinforma. Oxf. Engl. *20*, 307–315.
Gerriets, V.A., Kishton, R.J., Nichols, A.G., Macintyre, A.N., Inoue, M., Ilkayeva, O., Winter, P.S., Liu, X., Priyadharshini, B., Slawinska, M.E., et al. (2015). Metabolic programming and PDHK1 control CD4+ T cell subsets and inflammation. J. Clin. Invest. *125*, 194–207.
Geyer, P.E., Holdt, L.M., Teupser, D., and Mann, M. (2017). Revisiting biomarker discovery by plasma proteomics. Mol. Syst. Biol. *13*.
Granados, H.M., Ii, A.D., Tsurutani, N., Wright, K., Fernandez, M.L., Sylvester, F.A., and Vella, A.T. (2017). Programmed cell death-1, PD-1, is dysregulated in T cells from children with new onset type 1 diabetes. PLOS ONE *12*, e0183887.
Gustafsson, M., Gawel, D.R., Alfredsson, L., Baranzini, S., Björkander, J., Blomgran, R., Hellberg, S., Eklund, D., Ernerudh, J., Kockum, I., et al. (2015). A validated gene regulatory network and GWAS identifies early regulators of T cell-associated diseases. Sci. Transl. Med. *7*, 313ra178.
Han, F., Li, G., Dai, S., and Huang, J. (2016). Genome-wide metabolic model to improve understanding of CD4(+) T cell metabolism, immunometabolism and application in drug design. Mol. Biosyst. *12*, 431–443.
Hedegaard, C.J., Krakauer, M., Bendtzen, K., Lund, H., Sellebjerg, F., and Nielsen, C.H. (2008). T helper cell type 1 (Th1), Th2 and Th17 responses to myelin basic protein and disease activity in multiple sclerosis. Immunology *125*, 161–169.
Herring, T.A., Cuppett, S.L., and Zempleni, J. (2007). Genomic implications of H(2)O (2) for cell proliferation and growth of Caco-2 cells. Dig. Dis. Sci. *52*, 3005–3015.
Hoyer, K.K., Kuswanto, W.F., Gallo, E., and Abbas, A.K. (2009). Distinct roles of helper T-cell subsets in a systemic autoimmune disease. Blood *113*, 389–395.
Huang, D.W., Sherman, B.T., and Lempicki, R.A. (2009). Systematic and integrative analysis of large gene lists using DAVID bioinformatics resources. Nat. Protoc. *4*, 44–57.
Ivanova, E.A., and Orekhov, A.N. (2015). T Helper Lymphocyte Subsets and Plasticity in

Autoimmunity and Cancer: An Overview. BioMed Res. Int. *2015*, 327470.
Jerby, L., and Ruppin, E. (2012). Predicting Drug Targets and Biomarkers of Cancer via Genome-Scale Metabolic Modeling. Clin. Cancer Res. *18*, 5572–5584.
Jernås, M., Malmeström, C., Axelsson, M., Nookaew, I., Wadenvik, H., Lycke, J., and Olsson, B. (2013). MicroRNA regulate immune pathways in T-cells in multiple sclerosis (MS). BMC Immunol. *14*, 32.
Jin, Z., Mendu, S.K., and Birnir, B. (2013). GABA is an effective immunomodulatory molecule. Amino Acids *45*, 87–94.
Jones, D.E. (1996). T-cell autoimmunity in primary biliary cirrhosis. Clin. Sci. Lond. Engl. 1979 *91*, 551–558.
Kanehisa, M., Sato, Y., Kawashima, M., Furumichi, M., and Tanabe, M. (2016). KEGG as a reference resource for gene and protein annotation. Nucleic Acids Res. *44*, D457-462.
King, Z.A., Dräger, A., Ebrahim, A., Sonnenschein, N., Lewis, N.E., and Palsson, B.O. (2015). Escher: A Web Application for Building, Sharing, and Embedding Data-Rich Visualizations of Biological Pathways. PLOS Comput. Biol. *11*, e1004321.
Kleinewietfeld, M., Manzel, A., Titze, J., Kvakan, H., Yosef, N., Linker, R.A., Muller, D.N., and Hafler, D.A. (2013). Sodium chloride drives autoimmune disease by the induction of pathogenic TH17 cells. Nature *496*, 518–522.
Kumar, P., and Banik, S. (2013). Pharmacotherapy Options in Rheumatoid Arthritis. Clin. Med. Insights Arthritis Musculoskelet. Disord. *6*, 35–43.
Le Bourgeois, T., Strauss, L., Aksoylar, H.-I., Daneshmandi, S., Seth, P., Patsoukis, N., and Boussiotis, V.A. (2018). Targeting T Cell Metabolism for Improvement of Cancer Immunotherapy. Front. Oncol. *8*.
Li, E.K., Tam, L.-S., and Tomlinson, B. (2004). Leflunomide in the treatment of rheumatoid arthritis. Clin. Ther. *26*, 447–459.
Lian, G., Gnanaprakasam, J.R., Wang, T., Wu, R., Chen, X., Liu, L., Shen, Y., Yang, M., Yang, J., Chen, Y., et al. (2018). Glutathione de novo synthesis but not recycling process coordinates with glutamine catabolism to control redox homeostasis and directs murine T cell differentiation. ELife *7*.
Lü, S., Deng, J., Liu, H., Liu, B., Yang, J., Miao, Y., Li, J., Wang, N., Jiang, C., Xu, Q., et al. (2018). PKM2-dependent metabolic reprogramming in CD4+ T cells is crucial for hyperhomocysteinemia-accelerated atherosclerosis. J. Mol. Med. Berl. Ger. *96*, 585–600.
Lund, R., Aittokallio, T., Nevalainen, O., and Lahesmaa, R. (2003). Identification of novel genes regulated by IL-12, IL-4, or TGF-beta during the early polarization of CD4+ lymphocytes. J. Immunol. Baltim. Md 1950 *171*, 5328–5336.
Macintyre, A.N., Gerriets, V.A., Nichols, A.G., Michalek, R.D., Rudolph, M.C., Deoliveira, D., Anderson, S.M., Abel, E.D., Chen, B.J., Hale, L.P., et al. (2014). The glucose transporter Glut1 is selectively essential for CD4 T cell activation and effector function. Cell Metab. *20*, 61–72.
MacPherson, S., Horkoff, M., Gravel, C., Hoffmann, T., Zuber, J., and Lum, J.J. (2017). STAT3 Regulation of Citrate Synthase Is Essential during the Initiation of Lymphocyte Cell Growth. Cell Rep. *19*, 910–918.
Marks, R.E., Ho, A.W., Robbel, C., Kuna, T., Berk, S., and Gajewski, T.F. (2007). Farnesyltransferase inhibitors inhibit T-cell cytokine production at the posttranscriptional level. Blood *110*, 1982–1988.
Mathur, D., López-Rodas, G., Casanova, B., and Marti, M.B. (2014). Perturbed glucose metabolism: insights into multiple sclerosis pathogenesis. Front. Neurol. *5*, 250.
Mendu, S.K., Bhandage, A., Jin, Z., and Birnir, B. (2012). Different subtypes of GABA-A receptors are expressed in human, mouse and rat T lymphocytes. PloS One *7*, e42959.

Metzler, B., Gfeller, P., and Guinet, E. (2016). Restricting Glutamine or Glutamine-Dependent Purine and Pyrimidine Syntheses Promotes Human T Cells with High FOXP3 Expression and Regulatory Properties. J. Immunol. Baltim. Md 1950 *196*, 3618–3630.
Michalek, R.D., Gerriets, V.A., Jacobs, S.R., Macintyre, A.N., MacIver, N.J., Mason, E.F., Sullivan, S.A., Nichols, A.G., and Rathmell, J.C. (2011). Cutting edge: distinct glycolytic and lipid oxidative metabolic programs are essential for effector and regulatory CD4+ T cell subsets. J. Immunol. Baltim. Md 1950 *186*, 3299–3303.
Muri, J., Heer, S., Matsushita, M., Pohlmeier, L., Tortola, L., Fuhrer, T., Conrad, M., Zamboni, N., Kisielow, J., and Kopf, M. (2018). The thioredoxin-1 system is essential for fueling DNA synthesis during T-cell metabolic reprogramming and proliferation. Nat. Commun. *9*, 1851.
Nakagawa, R., Muroyama, R., Saeki, C., Goto, K., Kaise, Y., Koike, K., Nakano, M., Matsubara, Y., Takano, K., Ito, S., et al. (2017). miR-425 regulates inflammatory cytokine production in CD4+ T cells via N-Ras upregulation in primary biliary cholangitis. J. Hepatol. *66*, 1223–1230.
Okano, T., Saegusa, J., Takahashi, S., Ueda, Y., and Morinobu, A. (2018). Immunometabolism in rheumatoid arthritis. Immunol. Med. *41*, 89–97.
Osinalde, N., Mitxelena, J., Sánchez-Quiles, V., Akimov, V., Aloria, K., Arizmendi, J.M., Zubiaga, A.M., Blagoev, B., and Kratchmarova, I. (2016). Nuclear Phosphoproteomic Screen Uncovers ACLY as Mediator of IL-2-induced Proliferation of CD4+ T lymphocytes. Mol. Cell. Proteomics MCP *15*, 2076–2092.
Palmer, A.M. (2010). Teriflunomide, an inhibitor of dihydroorotate dehydrogenase for the potential oral treatment of multiple sclerosis. Curr. Opin. Investig. Drugs Lond. Engl. 2000 *11*, 1313–1323.
Patsoukis, N., Bardhan, K., Weaver, J., Herbel, C., Seth, P., Li, L., and Boussiotis, V.A. (2016). The role of metabolic reprogramming in T cell fate and function. Curr. Trends Immunol. *17*, 1–12.
Prots, I., Skapenko, A., Lipsky, P.E., and Schulze-Koops, H. (2011). Analysis of the transcriptional program of developing induced regulatory T cells. PloS One *6*, e16913.
Puniya, B.L., Kulshreshtha, D., Verma, S.P., Kumar, S., and Ramachandran, S. (2013). Integrated gene co-expression network analysis in the growth phase of Mycobacterium tuberculosis reveals new potential drug targets. Mol. Biosyst. *9*, 2798–2815.
Puniya, B.L., Allen, L., Hochfelder, C., Majumder, M., and Helikar, T. (2016a). Systems Perturbation Analysis of a Large-Scale Signal Transduction Model Reveals Potentially Influential Candidates for Cancer Therapeutics. Front. Bioeng. Biotechnol. *4*, 10.
Puniya, B.L., Kulshreshtha, D., Mittal, I., Mobeen, A., and Ramachandran, S. (2016b). Integration of Metabolic Modeling with Gene Co-expression Reveals Transcriptionally Programmed Reactions Explaining Robustness in *Mycobacterium tuberculosis*. Sci. Rep. *6*, 23440.
Puniya, B.L., Todd, R.G., Mohammed, A., Brown, D.M., Barberis, M., and Helikar, T. (2018). A Mechanistic Computational Model Reveals That Plasticity of CD4+ T Cell Differentiation Is a Function of Cytokine Composition and Dosage. Front. Physiol. *9*, 878.
Pushpakom, S., Iorio, F., Eyers, P.A., Escott, K.J., Hopper, S., Wells, A., Doig, A., Guilliams, T., Latimer, J., McNamee, C., et al. (2019). Drug repurposing: progress, challenges and recommendations. Nat. Rev. Drug Discov. *18*, 41–58.
Reimand, J., Isserlin, R., Voisin, V., Kucera, M., Tannus-Lopes, C., Rostamianfar, A., Wadi, L., Meyer, M., Wong, J., Xu, C., et al. (2019). Pathway enrichment analysis and visualization of omics data using g:Profiler, GSEA, Cytoscape and EnrichmentMap. Nat. Protoc. *14*, 482–517.
Reisdorf, W.C., Xie, Q., Zeng, X., Xie, W., Rajpal, N., Hoang, B., Burgert, M.E., Kumar, V., Hurle, M.R., Rajpal, D.K., et al. (2019). Preclinical evaluation of EPHX2 inhibition as a novel

treatment for inflammatory bowel disease. PloS One *14*, e0215033.
Ren, W., Liu, G., Yin, J., Tan, B., Wu, G., Bazer, F.W., Peng, Y., and Yin, Y. (2017). Amino-acid transporters in T-cell activation and differentiation. Cell Death Dis. *8*, e2757.
Rieckmann, J.C., Geiger, R., Hornburg, D., Wolf, T., Kveler, K., Jarrossay, D., Sallusto, F., Shen-Orr, S.S., Lanzavecchia, A., Mann, M., et al. (2017). Social network architecture of human immune cells unveiled by quantitative proteomics. Nat. Immunol. *18*, 583–593.
Ritchie, M.E., Phipson, B., Wu, D., Hu, Y., Law, C.W., Shi, W., and Smyth, G.K. (2015). limma powers differential expression analyses for RNA-sequencing and microarray studies. Nucleic Acids Res. *43*, e47.
Rongvaux, A., Galli, M., Denanglaire, S., Van Gool, F., Drèze, P.L., Szpirer, C., Bureau, F., Andris, F., and Leo, O. (2008). Nicotinamide phosphoribosyl transferase/pre-B cell colony-enhancing factor/visfatin is required for lymphocyte development and cellular resistance to genotoxic stress. J. Immunol. Baltim. Md 1950 *181*, 4685–4695.
Roulston, A., and Shore, G.C. (2016). New strategies to maximize therapeutic opportunities for NAMPT inhibitors in oncology. Mol. Cell. Oncol. *3*, e1052180.
Rowe, E., Palsson, B.O., and King, Z.A. (2018). Escher-FBA: a web application for interactive flux balance analysis. BMC Syst. Biol. *12*, 84.
Safran, M., Dalah, I., Alexander, J., Rosen, N., Iny Stein, T., Shmoish, M., Nativ, N., Bahir, I., Doniger, T., Krug, H., et al. (2010). GeneCards Version 3: the human gene integrator. Database J. Biol. Databases Curation *2010*, baq020.
Santarlasci, V., Maggi, L., Capone, M., Querci, V., Beltrame, L., Cavalieri, D., D'Aiuto, E., Cimaz, R., Nebbioso, A., Liotta, F., et al. (2012). Rarity of human T helper 17 cells is due to retinoic acid orphan receptor-dependent mechanisms that limit their expansion. Immunity *36*, 201–214.
Sayers, E.W., Agarwala, R., Bolton, E.E., Brister, J.R., Canese, K., Clark, K., Connor, R., Fiorini, N., Funk, K., Hefferon, T., et al. (2019). Database resources of the National Center for Biotechnology Information. Nucleic Acids Res. *47*, D23–D28.
Schweitzer, B.I., Dicker, A.P., and Bertino, J.R. (1990). Dihydrofolate reductase as a therapeutic target. FASEB J. Off. Publ. Fed. Am. Soc. Exp. Biol. *4*, 2441–2452.
Segrè, D., Vitkup, D., and Church, G.M. (2002). Analysis of optimality in natural and perturbed metabolic networks. Proc. Natl. Acad. Sci. U. S. A. *99*, 15112–15117.
Soria-Castro, R., Schcolnik-Cabrera, A., Rodríguez-López, G., Campillo-Navarro, M., Puebla-Osorio, N., Estrada-Parra, S., Estrada-García, I., Chacón-Salinas, R., and Chávez-Blanco, A.D. (2019). Exploring the Drug Repurposing Versatility of Valproic Acid as a Multifunctional Regulator of Innate and Adaptive Immune Cells. J. Immunol. Res. *2019*, 9678098.
Subramanian, A., Narayan, R., Corsello, S.M., Peck, D.D., Natoli, T.E., Lu, X., Gould, J., Davis, J.F., Tubelli, A.A., Asiedu, J.K., et al. (2017). A Next Generation Connectivity Map: L1000 Platform and the First 1,000,000 Profiles. Cell *171*, 1437-1452.e17.
Surls, J., Nazarov-Stoica, C., Kehl, M., Olsen, C., Casares, S., and Brumeanu, T.-D. (2012). Increased membrane cholesterol in lymphocytes diverts T-cells toward an inflammatory response. PloS One *7*, e38733.
Swainston, N., Smallbone, K., Hefzi, H., Dobson, P.D., Brewer, J., Hanscho, M., Zielinski, D.C., Ang, K.S., Gardiner, N.J., Gutierrez, J.M., et al. (2016). Recon 2.2: from reconstruction to model of human metabolism. Metabolomics Off. J. Metabolomic Soc. *12*, 109.
Szklarczyk, D., Morris, J.H., Cook, H., Kuhn, M., Wyder, S., Simonovic, M., Santos, A., Doncheva, N.T., Roth, A., Bork, P., et al. (2017). The STRING database in 2017: quality-controlled protein-protein association networks, made broadly accessible. Nucleic Acids

Res. *45*, D362–D368.
The Gene Ontology Consortium (2019). The Gene Ontology Resource: 20 years and still GOing strong. Nucleic Acids Res. *47*, D330–D338.
The UniProt Consortium (2017). UniProt: the universal protein knowledgebase. Nucleic Acids Res. *45*, D158–D169.
Tian, J., Yong, J., Dang, H., and Kaufman, D.L. (2011). Oral GABA treatment downregulates inflammatory responses in a mouse model of rheumatoid arthritis. Autoimmunity *44*, 465–470.
Wang, R., and Green, D.R. (2012). Metabolic reprogramming and metabolic dependency in T cells. Immunol. Rev. *249*, 14–26.
Wishart, D.S., Feunang, Y.D., Guo, A.C., Lo, E.J., Marcu, A., Grant, J.R., Sajed, T., Johnson, D., Li, C., Sayeeda, Z., et al. (2018). DrugBank 5.0: a major update to the DrugBank database for 2018. Nucleic Acids Res. *46*, D1074–D1082.
Xu, T., and Ding, S. (2017). Methods of treating disease by metabolic control of t-cell differentiation.
Yang, Z., Fujii, H., Mohan, S.V., Goronzy, J.J., and Weyand, C.M. (2013). Phosphofructokinase deficiency impairs ATP generation, autophagy, and redox balance in rheumatoid arthritis T cells. J. Exp. Med. *210*, 2119–2134.
Yang, Z., Matteson, E.L., Goronzy, J.J., and Weyand, C.M. (2015). T-cell metabolism in autoimmune disease. Arthritis Res. Ther. *17*.
Ye, H., Zhang, J., Wang, J., Gao, Y., Du, Y., Li, C., Deng, M., Guo, J., and Li, Z. (2015). CD4 T-cell transcriptome analysis reveals aberrant regulation of STAT3 and Wnt signaling pathways in rheumatoid arthritis: evidence from a case-control study. Arthritis Res. Ther. *17*, 76.
Yin, Y., Choi, S.-C., Xu, Z., Perry, D.J., Seay, H., Croker, B.P., Sobel, E.S., Brusko, T.M., and Morel, L. (2015). Normalization of CD4+ T cell metabolism reverses lupus. Sci. Transl. Med. *7*, 274ra18.
Yin, Y., Choi, S.-C., Xu, Z., Zeumer, L., Kanda, N., Croker, B.P., and Morel, L. (2016). Glucose Oxidation Is Critical for CD4+ T Cell Activation in a Mouse Model of Systemic Lupus Erythematosus. J. Immunol. Baltim. Md 1950 *196*, 80–90.
Young, K.E., Flaherty, S., Woodman, K.M., Sharma-Walia, N., and Reynolds, J.M. (2017). Fatty acid synthase regulates the pathogenicity of Th17 cells. J. Leukoc. Biol. *102*, 1229–1235.
Zhang, H., Nestor, C.E., Zhao, S., Lentini, A., Bohle, B., Benson, M., and Wang, H. (2013). Profiling of human CD4+ T-cell subsets identifies the TH2-specific noncoding RNA GATA3-AS1. J. Allergy Clin. Immunol. *132*, 1005–1008.
Zhu, J., and Paul, W.E. (2008). CD4 T cells: fates, functions, and faults. Blood *112*, 1557–1569.

Competing Interests

The authors declare that they have no conflict of interest.

Acknowledgements

This work was supported by NIH grant 1R35GM119770-04 to T.H. and by the Systems Biology

Grant of the University of Surrey to M.B.

Author Contributions

B.L.P., M.B., and T.H. conceived and designed the study. B.L.P., M.B., and T.H. defined the pipeline to integrate -omics data, and B.L.P implemented the pipeline. B.L.P. and B.L. performed literature mining. B.L.P., B.L., R.M., A.C., and S.T. collected the data. B.L.P., B.L., R.M., and A.C. constructed the models. A.R.S. performed refinement of the constructed models. B.L.P., B.L., R.M., A.C., S.T., M.B., and T.H. analyzed the data. B.L.P., M.B., and T.H. wrote the manuscript. M.B. and T.H. supervised the study.

Availability of data and materials

The models generated in this study are available in the supplementary files and can also be accessed from the biomodels database under accession MODEL1909260003, MODEL1909260004, MODEL1909260005, MODEL1909260006. The scripts used in this pipeline are available from the corresponding author on reasonable request.

Tables

Table 1: Metabolic models of CD4+ T cells

	Naïve	**Th1**	**Th2**	**Th17**
Genes	1055	1133	1127	1250
Reactions	5179	3956	5252	5282
Internal reactions (Enzyme catalyzed)	2501	1969	2549	2640
Metabolites	3153	2517	3156	3263

Table 2: Identified CD4+ T cell drug targets for RA, MS, and PBC

Disease	**Entrez ID**	**Gene Symbol**	**Gene description**	**Aggregate Z-score**	**Literature evidences relevant to CD4+ T cells and autoimmune diseases**	**ChEMBL (Gaulton et al., 2017)IDs***

RA	4047	LSS	Lanosterol synthase	-3.35	Inhibition of lanosterol synthase (LSS) might decrease the endogenous cholesterol that may lead to impact cell division (Herring et al., 2007).	CHEMBL3593
	18	ABAT	4-aminobutyrate aminotransferase	-3.20	GABA downregulate inflammatory response in a mouse model of RA (Tian et al., 2011); Inhibition of ABAT might increase GABA (Soria-Castro et al., 2019).	CHEMBL2044
	10135	NAMPT	Nicotinamide phosphoribosyltransferase	-3.11	Nampt inhibition reduces demyelination and disability in EAE (Bruzzone et al., 2009)), Lack of NAMPT expression affect T cell development (Rongvaux et al., 2008).	CHEMBL1744525
	2224	FDPS	Farnesyl pyrophosphate synthase	-2.98	Inhibition of FDPS inhibit T cell cytokine production (Marks et al., 2007).	CHEMBL1782
	6713	SQLE	Squalene monooxygenase	-2.96	Increased Membrane Cholesterol in T cells leads to inflammatory response (Surls et al., 2012).	CHEMBL3592
	2222	FDFT1	Farnesyl-diphosphate farnesyltransferase	-2.66	No support	CHEMBL3338
	2053	EPHX2	Bifunctional epoxide hydrolase 2	-2.44	Inhibition of EPHX2 pre clinically evaluated as drug target for IBD (Reisdorf et al., 2019).	CHEMBL2409
	4967	OGDH	2-oxoglutarate dehydrogenase	-2.30	No support	CHEMBL2816
	847	CAT	Catalase	-2.22	Protect T cells against oxidative stress (Ando et al., 2008).	CHEMBL3627594
	1431	CS	Citrate synthase	-2.17	Inhibition of citrate synthase leads to reduction in citrate leading to reduced proliferation (MacPherson et al., 2017).	DB02637
	5162	PDHB	Pyruvate dehydrogenase E1 component subunit beta	-2.04	No support	DB00119
	1312	COMT	Catechol O-methyltransferase	-1.80	No support	CHEMBL2023
	26275	HIBCH	3-hydroxyisobutyryl-CoA hydrolase	-1.73	No support	CHEMBL3817723
	6648	SOD2	Superoxide dismutase [Mn], mitochondrial	-1.32	Loss of SOD2 increased superoxide, and defective T cell development (Case et al., 2011).	CHEMBL4105776
	1723	DHODH	Dihydroorotate dehydrogenase	-1.26	Explored as a potential drug target for RA (Breedveld and Dayer, 2000) and MS (Palmer, 2010).	CHEMBL1966
	2548	GAA	alpha-glucosidase	-1.06	No support	CHEMBL2608
	38	ACAT1	Acetyl-CoA acetyltransferase, mitochondrial	-1.01	Target of Sulfasalazine that is anti inflammatory indicated for treatment of ulcerative colitis and rheumatoid arthritis (Wishart et al., 2018).	CHEMBL2616
MS	1376	CPT2	Carnitine O-palmitoyltransferase 2	-3.09	No support	CHEMBL3238
	847	CAT	Catalase	-3.08	Protect T cells against oxidative stress (Ando et al., 2008).	CHEMBL3627594
	498	ATP5F1A	ATP synthase subunit alpha	-3.04	No support	CHEMBL2062351
	506	ATP5F1B	ATP synthase subunit beta	-2.88	No support	CHEMBL2062350
	509	ATP5F1C	ATP synthase F1 subunit gamma	-2.71	No support	DB04216
	4953	ODC1	Ornithine decarboxylase	-2.67	No support	CHEMBL1869
	471	ATIC	MP cyclohydrolase	-2.66	No support	CHEMBL3430882
	513	ATP5F1D	ATP synthase subunit delta	-2.55	No support	DB00228
	515	ATP5PB	ATP synthase F(0) complex subunit B1	-2.39	No support	BTB06584 (cMap)
	128	ADH5	Alcohol dehydrogenase class-3	-2.19	No support	CHEMBL4116
	1806	DPYD	Dihydropyrimidine dehydrogenase	-1.83	No support	CHEMBL3172
	3418	IDH2	Isocitrate dehydrogenase	-1.61	knockdown of IDHl or IDH2 reduces IL-17 producing cells (Patent WO2017123808A1) (Xu and Ding, 2017).	CHEMBL3991501
	2936	GSR	Glutathione reductase	-1.59	Inhibition of GSH de novo synthesis reduce the pathological progression of EAE (Lian et al., 2018).	DB0262
	3156	HMGCR	3-hydroxy-3-methylglutaryl-coenzyme A reductase	-1.58	Potential target for autoimmune diseases (Arefieva et al., 2018).	CHEMBL402

	2222	FDFT1	Farnesyl-diphosphate farnesyltransferase	-1.55	No support	CHEMBL3338
	1719	DHFR	Dihydrofolate reductase	-1.52	Low dose Methotrexate (inhibitor of DHFR) found effective for MS, RA, and Crohn's disease (Ashtari and Savoj, 2011).	CHEMBL202
	5315	PKM	Pyruvate kinase	-1.51	Potential target to regulate inflammation (Alves-Filho and Pålsson-McDermott, 2016).	CHEMBL1075189
	2618	GART	phosphoribosylglycinamide formyltransferase	-1.46	No support	CHEMBL3972
	18	ABAT	4-aminobutyrate aminotransferase	-1.41	GABA downregulate inflammatory response in mouse model of RA (Tian et al., 2011); Inhibition of ABAT might increase GABA (Soria-Castro et al., 2019).	CHEMBL2044
	4047	LSS	Lanosterol synthase	-1.28	Inhibition of lanosterol synthase (LSS) might decrease the endogenous cholesterol that may lead to impact cell division (Herring et al., 2007).	CHEMBL3593
	2194	FASN	Fatty acid synthase	-1.16	Fatty acid synthase linked to pathogenicity of Th17 cells (Young et al., 2017) .	CHEMBL4106134
	5471	PPAT	phosphoribosyl pyrophosphate amidotransferase	-1.15	Knock down of CAD and PPAT promotes regulatory CD4+ T cells (Metzler et al., 2016).	CHEMBL2362992
	4860	PNP	Purine nucleoside phosphorylase	-1.12	inhibition leads to T cell suppression (Bantia and Kilpatrick, 2004).	CHEMBL4338
	1431	CS	Citrate synthase	-1.11	Increased Citrate in MS patients (Mathur et al., 2014).	DB02637
	293	SLC25A6	ADP/ATP translocase 3	-1.11	No support	CHEMBL4105854
	790	CAD	carbamoyl-phosphate synthetase 2	-1.03	Knock down of CAD and PPAT promotes regulatory CD4+ T cells (Metzler et al., 2016).	CHEMBL3093
	6713	SQLE	Squalene monooxygenase	-1.00	Increased Membrane Cholesterol in T cells leads to inflammatory response (Surls et al., 2012).	CHEMBL3592
PBC	10135	NAMPT	Nicotinamide phosphoribosyltransferase	-6.10	Nampt inhibition reduces demyelination and disability in EAE (Bruzzone et al., 2009), Lack of NAMPT expression affect T cell development (Rongvaux et al., 2008).	CHEMBL1744525
	3704	ITPA	Inosine triphosphate pyrophosphatase	-5.31	No support	CHEMBL4105788
	132	ADK	Adenosine kinase	-4.90	No support	CHEMBL3589
	2181	ACSL3	Long-chain-fatty-acid--CoA ligase 3	-4.42	No support	DB00159
	1890	TYMP	Thymidine phosphorylase	-4.13	No support	CHEMBL3106
	262	AMD1	S-adenosylmethionine decarboxylase proenzyme	-4.04	No support	CHEMBL4181
	353	APRT	Adenine phosphoribosyltransferase	-3.89	No support	CHEMBL4105819
	128	ADH5	Alcohol dehydrogenase class-3	-3.89	No support	CHEMBL4116
	1312	COMT	Catechol O-methyltransferase	-3.71	No support	CHEMBL2023
	2053	EPHX2	Bifunctional epoxide hydrolase 2	-3.64	Inhibition of EPHX2 pre clinically evaluated as drug target for IBD (Reisdorf et al., 2019).	CHEMBL2409
	26275	HIBCH	3-hydroxyisobutyryl-CoA hydrolase	-3.64	No support	CHEMBL3817723
	2194	FASN	Fatty acid synthase	-3.62	Fatty acid synthase linked to pathogenicity of Th17 cells (Young et al., 2017) .	CHEMBL4106134
	2720	GLB1	Beta-galactosidase	-3.56	No support	CHEMBL2522
	114971	PTPMT1	Phosphatidylglycerophosphatase and protein-tyrosine phosphatase 1	-3.28	No support	CHEMBL2052033
	100	ADA	Adenosine deaminase	-3.15	ADA is a potential target for treatment of inflammatory disorders (Antonioli et al., 2012).	CHEMBL1910
	2739	GLO1	Lactoylglutathione lyase	-3.10	No support	CHEMBL2424
	2539	G6PD	Glucose-6-phosphate 1-dehydrogenase	-3.06	No support	CHEMBL5347
	3251	HPRT1	Hypoxanthine-guanine phosphoribosyltransferase	-2.97	No support	CHEMBL3243916

	2548	GAA	alpha-glucosidase	-2.96	No support	CHEMBL2608
	6515	SLC2A3	Solute carrier family 2, facilitated glucose transporter member 3	-2.51	Glut3 expressed in differentiated cells and resting equals to glut1 (Macintyre et al., 2014).	CHEMBL5215
	4363	ABCC1	Multidrug resistance-associated protein 1	-2.31	No support	CHEMBL3004
	7296	TXNRD1	Thioredoxin reductase 1	-1.99	essential for DNA synthesis during T-cell metabolic reprogramming and proliferation (Muri et al., 2018).	CHEMBL1927
	6647	SOD1	Superoxide dismutase	-1.67	No support	CHEMBL2354
	47	ACLY	ATP-citrate synthase	-1.57	Inactivation of ACLY reduces IL-2-promoted CD4+ T-cell growth (Osinalde et al., 2016).	CHEMBL3720

*In cases where ChEMBL ids were not available DrugBank (Wishart et al., 2018) ids of molecules or name of molecule provided as given in repurposing tool of cMap database.

Table 3: Drugs and compounds for identified drug targets

Gene Symbol	Gene description	Drugs/ compound*	Status of drugs/Compounds*
LSS	Lanosterol synthase	R0-48-8071	Preclinical
ABAT	4-aminobutyrate aminotransferase	Vigabatrin, Phenelzine, valproic acid	launched
NAMPT	Nicotinamide phosphoribosyltransferase	FK866	Phase 2
FDPS	Farnesyl pyrophosphate synthase	Pamidronic acid, Zoledronic acid, Alendronic acid, Ibandronate, Risedronic acid	Launched
SQLE	Squalene monooxygenase	Ellagic-acid	Phase 2
FDFT1	Farnesyl-diphosphate farnesyltransferase	TAK-475	Investigational
EPHX2	Bifunctional epoxide hydrolase 2	GSK2256294A	Phase 1
OGDH	2-oxoglutarate dehydrogenase	Valproic acid	Launched
CAT	Catalase	Fomepizole	Launched
CS	Citrate synthase	Oxaloacetate	Phase 2/ Phase 3
PDHB	Pyruvate dehydrogenase E1 component subunit beta	2-oxopropanoate	Preclinical
COMT	Catechol O-methyltransferase	Entacapone, Nitecapone, Opicapone	Launched, Phase 2, phase 3
HIBCH	3-hydroxyisobutyryl-CoA hydrolase	Quercetin	Launched
SOD2	Superoxide dismutase [Mn], mitochondrial	Tetraethylenepentamine	Phase 2/ Phase 3
DHODH	Dihydroorotate dehydrogenase	Atovaquone, Leflunomide, Teriflunomide, Brequinar	Launched
GAA	alpha-glucosidase	Miglitol, Acarbose	Launched
ACAT1	Acetyl-CoA acetyltransferase, mitochondrial	Sulfasalazine	Launched
CPT2	Carnitine O-palmitoyltransferase 2	Perhexiline	Launched
ATP5F1A	ATP synthase subunit alpha	Quercetin	Launched,
ATP5F1B	ATP synthase subunit beta	Quercetin	Launched
ATP5F1C	ATP synthase F1 subunit gamma	Quercetin	Launched
ODC1	Ornithine decarboxylase	MC-1, Putrescine	Phase 3, Phase 2
ATIC	MP cyclohydrolase	Pemetrexed	Launched

ATP5F1D	ATP synthase subunit delta	Sevoflurane, Enflurane, Methoxyflurane	Launched
ATP5PB	ATP synthase F(0) complex subunit B1	BTB06584	Preclinical
ADH5	Alcohol dehydrogenase class-3	N6022	Phase 1/Phase 2
DPYD	Dihydropyrimidine dehydrogenase	5-fluorouracil, Gimeraci	Launched
IDH2	Isocitrate dehydrogenase	AGI-6780	Preclinical
GSR	Glutathione reductase	Carmustine	Launched
HMGCR	3-hydroxy-3-methylglutaryl-coenzyme A reductase	Atorvastatin, Fluvastatin, Lovastatin, Meglutol, Pitavastatin, Pravastatin, Rosuvastatin, Simvastatin, Nadide	Launched
DHFR	Dihydrofolate reductase	Aminopterin, Chlorproguanil, Methotrexate, Pralatrexate, Proguanil, Pyrimethamine, Sulfameter, Trimethoprim, Pemetrexed	Launched
PKM	Pyruvate kinase	TEPP-46, 2-oxopropanoate	Preclinical
GART	phosphoribosylglycinamide formyltransferase	Pemetrexed	Launched
FASN	Fatty acid synthase	Pyrazinamide, Cerulenin	Launched
PPAT	phosphoribosyl pyrophosphate amidotransferase	Azathioprine, Mercaptopurine	Launched
PNP	Purine nucleoside phosphorylase	Acyclovir, Didanosine	Launched
SLC25A6	ADP/ATP translocase 3	Clodronic-acid	Launched
CAD	carbamoyl-phosphate synthetase 2	Sparfosate	Phase 3
ITPA	Inosine triphosphate pyrophosphatase	Citric-acid	Preclinical
ADK	Adenosine kinase	ABT-702	Preclinical
ACSL3	Long-chain-fatty-acid--CoA ligase 3	Icosapent	Launched
TYMP	Thymidine phosphorylase	Tipiracil	Launched
AMD1	S-adenosylmethionine decarboxylase proenzyme	Ademetionine, Putrescine	Launched, Phase 2
APRT	Adenine phosphoribosyltransferase	Citric-acid	Preclinical
GLB1	Beta-galactosidase	Fagomine	Phase 2
PTPMT1	Phosphatidylglycerophosphatase and protein-tyrosine phosphatase 1	Alexidine	Preclinical
ADA	Adenosine deaminase	Cladribine, Pentostatin, Dipyridamole, Fludarabine	Launched
GLO1	Lactoylglutathione lyase	Indomethacin	Launched
G6PD	Glucose-6-phosphate 1-dehydrogenase	RRx-001	Phase 2
HPRT1	Hypoxanthine-guanine phosphoribosyltransferase	Azathioprine, Mercaptopurine	Launched
SLC2A3	Solute carrier family 2, facilitated glucose transporter member 3	2-deoxyglucose	Phase 2
ABCC1	Multidrug resistance-associated protein 1	Reversan, Ko143	Preclinical
TXNRD1	Thioredoxin reductase 1	Fotemustine	Launched
SOD1	Superoxide dismutase	Tetraethylenepentamine	Phase 2/Phase 3
ACLY	ATP-citrate synthase	ETC-1002	Phase 3

* Data obtained from repurposing tool (Corsello et al., 2017) of cMap database and DrugBank (Wishart et al., 2018).

Figures and Figure Legends

Fig. 1

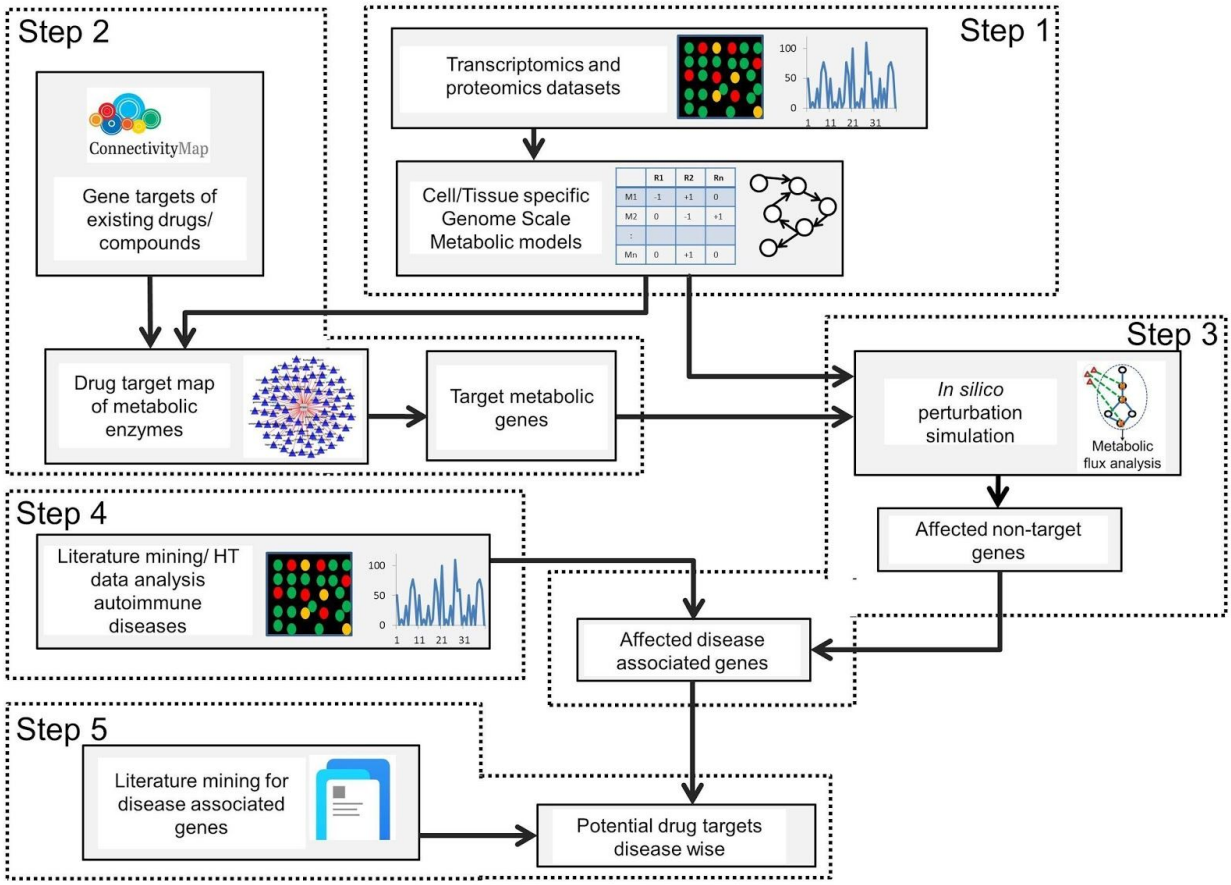

Fig. 1. Integrative approach for the identification of potential metabolic drug targets

The computational approach comprised of five major steps: (1) Construction of metabolic models using integrated transcriptomics and proteomics data, (2) Identification of metabolic

genes that are targets for existing drugs/compounds, (3) *In silico* inhibition of targets of existing drugs to identify affected reactions, (4) Identification of integrating differentially expressed genes (DEGs) in autoimmune diseases and integration with flux ratios obtained by perturbed and WT flux comparisons, and (5) Validation with literature and prediction of new targets.

Fig. 2

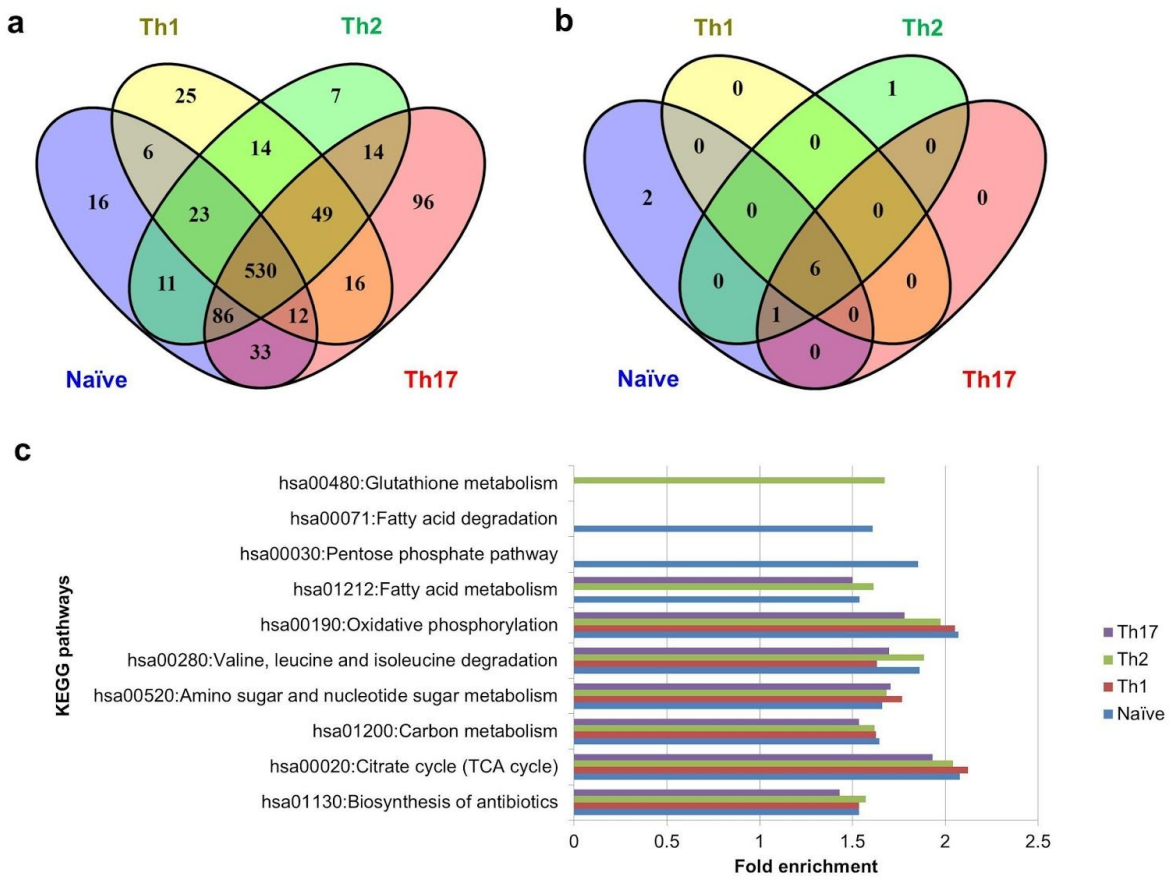

Fig 2. Construction of metabolic models in CD4+ T cells

(a) Active metabolic genes identified using transcriptomics and proteomics data of CD4+ T cell subtypes. (b) KEGG pathway enrichment analysis of active genes in each cell type using all

1,892 metabolic genes as a background. (c) Fold enrichment of KEGG pathways enriched across CD4+ T cell subtypes.

Fig. 3

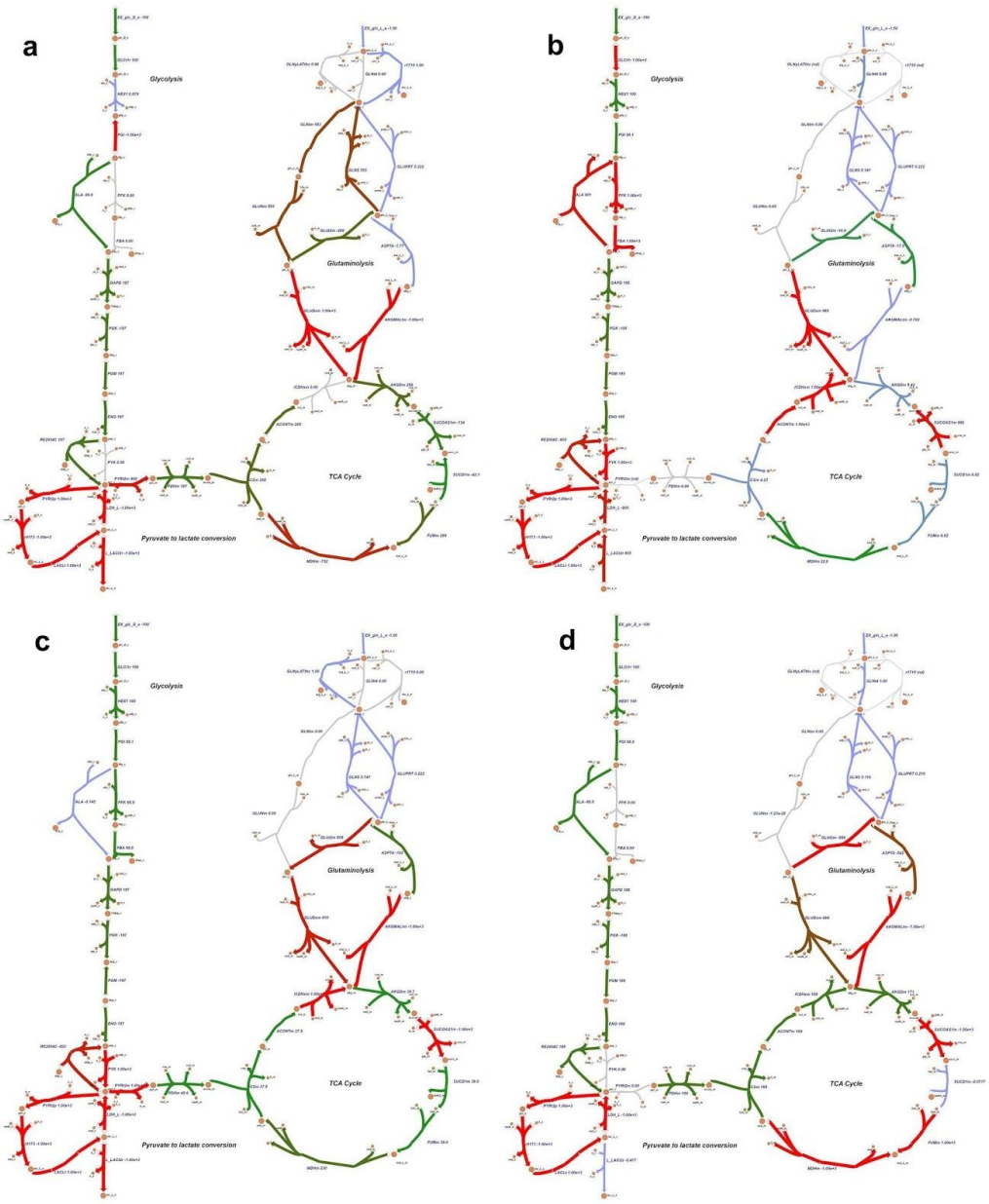

Fig 3. Flux maps of metabolic pathways active in CD4+ T cell metabolic models

Escher maps showing fluxes through glycolysis, glucose to lactate conversion, TCA cycle, glutaminolysis in naïve (a), Th1 (b), Th2 (c), and Th17 (d) models. All the models convert pyruvate to lactate (aerobic glycolysis). In glycolysis, naïve model had the reverse direction flux

through PGI reaction while effector cells have forward direction flux. All the models uptake glutamine that ultimately forms α-Ketoglutaric acid (glutaminolysis). GLNtm (glutamine transporter) and GLUNm (convert glutamine to glutamate) reactions are active in naïve model and not in effector CD4+ T cell models that use different routes for glutamine to glutamate conversion.

Fig. 4

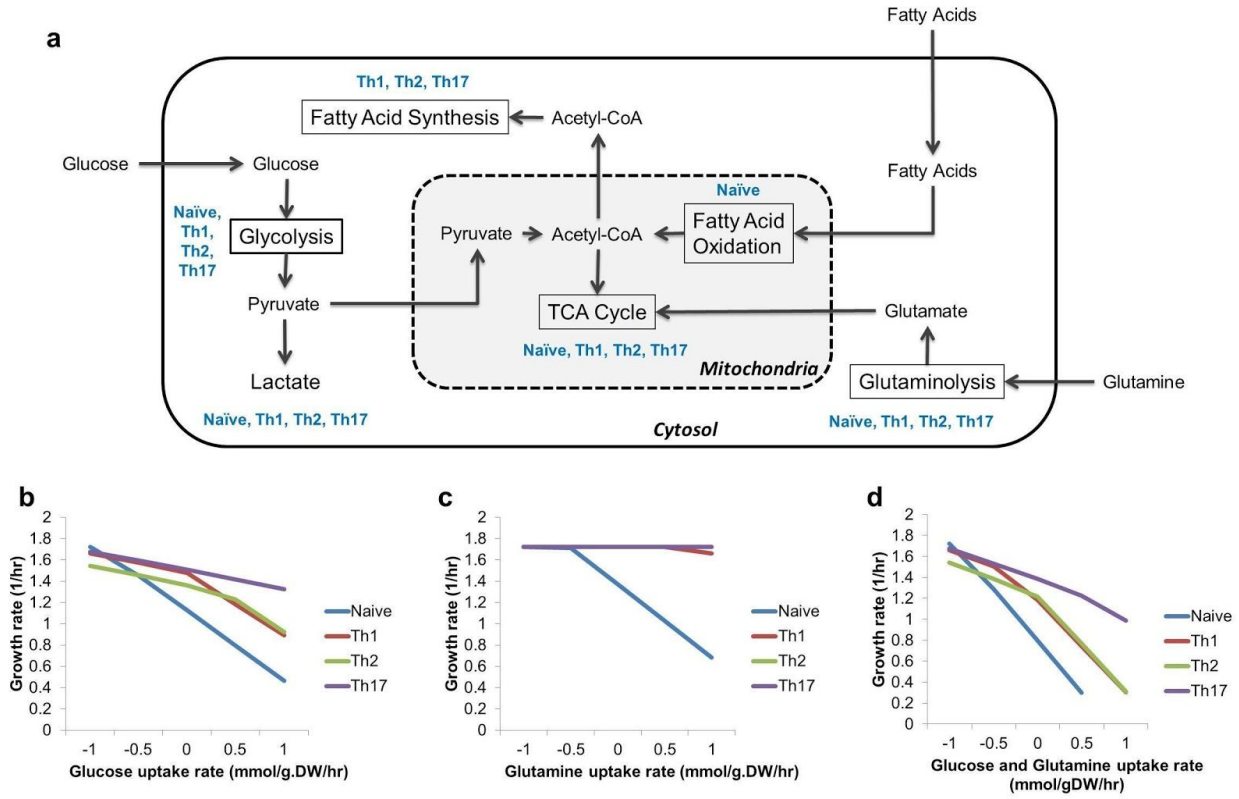

Fig. 4: Validation of metabolic models

(a) Summary of active pathways in the CD4+ T cell subtypes that are in agreement of literature. The activity of pathways in a model was determined by *Flux Balance Analysis*. The pathways

shown in the box are active in CD4+ T cell subtypes models, and blue color is used to indicate the specific CD4+ T cell subtype. For example, the glycolysis pathway is active in all five T cell models. (b, c, and d) The dependency of growth rate (in all models) on glucose (b), glutamine (c), and on both glucose and glutamine (d).

Fig. 5

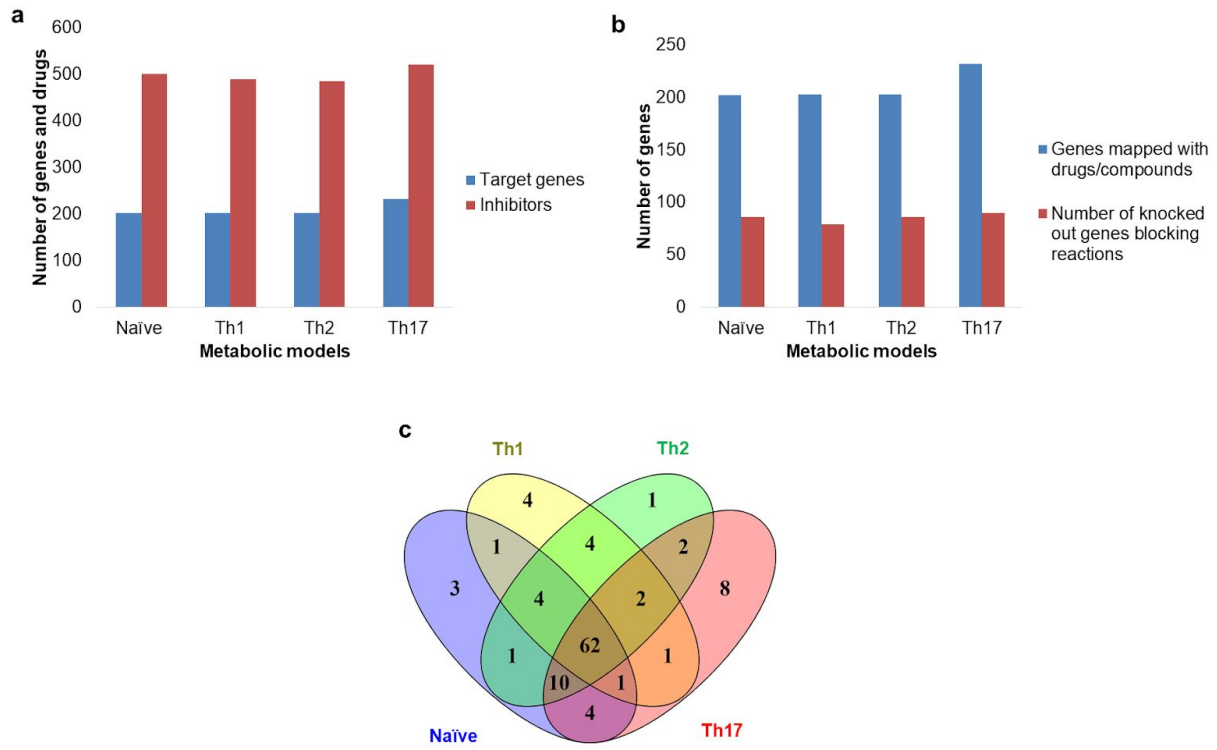

Fig. 5: Drug targets in CD4+ T cell models

(a) Distribution of metabolic drug target genes, and inhibitory drugs or compounds in each model. (b) Number of metabolic genes in the models mapped with inhibitory drugs (blue bars) and number of genes among drugs mapped genes that can block at least one reaction upon

inhibition (red bars). (c) Comparison of metabolic drug targets that affect reactions upon deletion in CD4+ T cell models.

Fig. 6

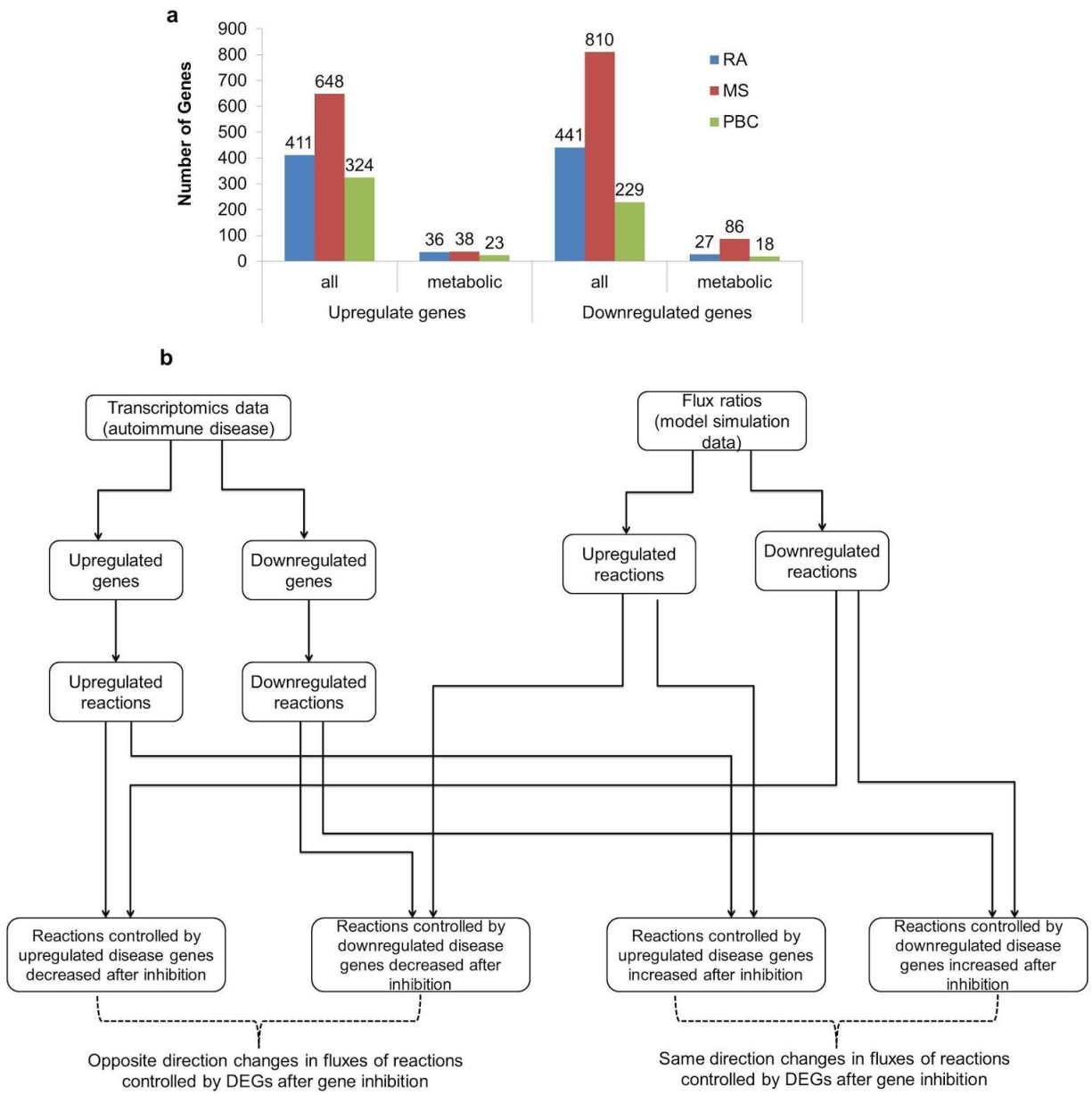

Fig. 6: Identification of potential drug targets for RA, MS, and PBC

(a) Number of all differentially expressed genes (DEGs) and metabolic DEGs in three diseases rheumatoid arthritis (RA), multiple sclerosis (MS), and primary biliary cholangitis (PBC). The DEGs were analyzed using three transcriptomics datasets (one dataset per disease). The data were obtained from peripheral CD4+ T cells of groups of patients and healthy individuals. (b)

Schematic representation of the integration of disease-associated differentially expressed genes and affected reaction on each drug target gene perturbation. For each drug target deletion, we investigated how many of fluxes regulated by upregulated genes are decreased and fluxes regulated by downregulated by increased. We used these numbers to calculate PES (perturbation effect score, *see STAR Methods*).